



Kamsri, P., Punkvang, A., Hannongbua, S., Suttisintong, K., Kittakoo, P., Spencer, J., Mulholland, A. J., & Pungpo, P. (2019). In silico study directed towards identification of the key structural features of GyrB inhibitors targeting MTB DNA gyrase: HQSAR, CoMSIA and molecular dynamics simulations. *SAR and QSAR in Environmental Research*, 30(11), 775-800.
<https://doi.org/10.1080/1062936X.2019.1658218>

Peer reviewed version

Link to published version (if available):
[10.1080/1062936X.2019.1658218](https://doi.org/10.1080/1062936X.2019.1658218)

[Link to publication record in Explore Bristol Research](#)
PDF-document

This is the author accepted manuscript (AAM). The final published version (version of record) is available online via Taylor & Francis at <https://www.tandfonline.com/doi/full/10.1080/1062936X.2019.1658218> . Please refer to any applicable terms of use of the publisher.

University of Bristol - Explore Bristol Research

General rights

This document is made available in accordance with publisher policies. Please cite only the published version using the reference above. Full terms of use are available:
<http://www.bristol.ac.uk/red/research-policy/pure/user-guides/ebr-terms/>

1 ***In silico* Study Directed Towards Identification the Key Structural**
2 **Feature of GyrB Inhibitors Targeting MTB DNA Gyrase: HQSAR,**
3 **CoMSIA and Molecular Dynamics Simulations**

4 Pharit Kamsri^{a,*}, Auradee Punkvang^a, Supa Hannongbua^b, Khomson
5 Suttisintong^c, Prasat Kittakoop^{d,e,f}, James Spencer^g, Adrian J. Mulholland^h,
6 and Pornpan Pungpoⁱ

7 *^aDivision of Chemistry, Faculty of Science, Nakhon Phanom University, Nakhon*
8 *Phanon, Thailand; ^bDepartment of Chemistry, Faculty of Science, Kasetsart University,*
9 *Bangkok, Thailand; ^cNational Nanotechnology Center, NSTDA, Pathum Thani,*
10 *Thailand; ^d Chulabhorn Research Institute, Bangkok, Thailand; ^e Chulabhorn Graduate*
11 *Institute, Chemical Biology Program, Chulabhorn Royal Academy, Bangkok, Thailand;*
12 *^fCenter of Excellence on Environmental Health and Toxicology (EHT), CHE, Ministry*
13 *of Education, Bangkok, Thailand ; ^gSchool of Cellular and Molecular Medicine,*
14 *University of Bristol, Bristol, U.K.; ^hCentre for Computational Chemistry, School of*
15 *Chemistry, University of Bristol, Bristol, U.K.; ⁱDepartment of Chemistry, Faculty of*
16 *Science, Ubon Ratchathani University, Ubon Ratchathani, Thailand*

17
18 ***Corresponding authors**

19 ^aPharit Kamsri
20 Division of Chemistry, Faculty of Science,
21 Nakhon Phanom University,
22 Nakhon Phanom, Thailand
23 E-mail: pharit.kamsri@npu.ac.th
24 Tel: +664 2503 776

***In silico* Study Directed Towards Identification the Key Structural Feature of GyrB Inhibitors Targeting MTB DNA Gyrase: HQSAR, CoMSIA and Molecular Dynamics Simulations**

MTB DNA gyrase subunit B (GyrB) has been identified as promising target for rational drug design against fluoroquinolone drug resistant tuberculosis. In this study, we attempted to identify the key structural feature for highly potent GyrB inhibitors through 2D-QSAR using HQSAR, 3D-QSAR using CoMISA and MD simulations approaches on a series of thiazole urea core derivatives. The best HQSAR and CoMSIA models based on IC₅₀ and MIC displayed the structural basis required for good activity against both GyrB enzyme and mycobacterial cell. MD simulations and binding free energy analysis using MM-GBSA and waterswap calculations revealed that urea core of inhibitors has strongest interaction with Asp79 via hydrogen bond interactions. In addition, cation-pi interaction and hydrophobic interactions of R₂ substituent with Arg82 and Arg141 help to enhance the binding affinity in GyrB ATPase binding site. Thus, the present study beneficially provides crucial structural feature and a structural concept for rational design of novel DNA gyrase inhibitors with improved biological activities against both enzyme and mycobacterial cell; good pharmacokinetic properties and drug safely profiles.

Keywords: GyrB inhibitors; Binding free energy; CoMSIA; HQSAR; MD simulations, DNA gyrase

Introduction

Tuberculosis, TB caused by *Mycobacterium tuberculosis* (MTB) is one of the top 10 causes of death worldwide and the leading cause from a single infectious agent. There are 1.6 million deaths and 10.0 million people developed TB disease in 2017 [1]. [Based on drug resistant tuberculosis, potential targets for tuberculosis drug development have been validated \[2-4\].](#) DNA gyrase had been identified as potential target for anti-tuberculosis drug discovery and the attractive target of fluoroquinolones, second-line drug for multidrug resistant tuberculosis (MDR-TB) [5-9]. This enzyme involved in the DNA replication mechanism. DNA gyrase consisted two subunits, DNA gyrase subunit A (GyrA) and DNA gyrase subunit B (GyrB) domains, in the holoenzyme complex as a heterotetramer A₂B₂ [10-12]. Only GyrA interacted with DNA and did the DNA cleavage

1 and relegation processes by tyrosine residue in the catalytic site [13,14], whereas the
2 GyrB promoted the ATP hydrolysis to process the catalytic cycles [15]. Fluroquinolone
3 drugs interacted with DNA in GyrA domain to create conformational changes of DNA
4 gyrase enzyme [5]. However, resistance to fluoroquinolones may occur spontaneously
5 due to the mutation of fluoroquinolone binding site leading to extensively drug resistant
6 tuberculosis (XDR-TB) [16-19]. To overcome fluoroquinolone drug resistant, novel
7 DNA gyrase inhibitors which shown the alternative inhibition mechanism at the ATPase
8 binding site of GyrB were proposed [7-9] such as 4-aminoquinolines [20], thiazole–
9 aminopiperidines [21], pyrrolamides [22], 2-amino-5-phenylthiophene-3-carboxamides
10 [23], quinoline–aminopiperidines [24], benzofurans [25] and benzo[*d*]isothiazoles [26].
11 Thiazole urea cores derivatives [27, 28] were discovered as GyrB inhibitors by a scaffold-
12 hopping approach. Some compounds showed good potency against GyrB enzyme and *M.*
13 *tuberculosis* with high correlation between GyrB inhibitory activity and anti-microbial
14 activity. Based on the promising results from this report, lead optimization process was
15 required. However, these compounds show low pharmacokinetic properties. The
16 optimization of thiazole urea derivatives to build good pharmacokinetic properties and
17 safety profile were required. Recently, QSAR study have been applied to identify the
18 structural requirement of DNA gyrase inhibitors including fluoroquinolone [29-31],
19 isothiazoloquinolone [31] and quinoline-aminopiperidine [32] derivatives. However,
20 information of the key structural features of inhibitors responsible to both enzyme and
21 bacterial cell inhibition were not reported. In the present study, QSAR approaches and
22 MD simulations were performed to gain insight into the key structural features of thiazole
23 urea core derivatives responsible to GyrB and mycobacterial inhibitions. The obtained
24 results revealed the key structural structure that serve as template in designing for high
25 potency of DNA gyrase inhibitors. The finding concept in the present study were applied
26 to design novel thiazole urea derivatives. In addition, pharmacokinetic properties of novel
27 designed thiazole urea derivatives were considered. Compounds with high predictions of
28 GyrB enzyme inhibition and mycobacterial inhibition that showed good pharmacokinetic
29 properties were proposed.

1 **Material and Methods**

2 *Compound dataset*

3 55 thiazole urea core derivatives including thiazolopyridinone urea,
4 thiazolopyridine urea and benzothiazole urea derivatives (Table 1) with GyrB ATPase
5 inhibition activity (inhibition concentration of compound required for ATPase inhibition
6 activity at 50% (IC₅₀) in nanomolar concentration unit) and anti-mycobacterial activity
7 (minimum inhibitory concentration (MIC) in micromolar concentration unit) were
8 collected from the literature [27, 28]. The general scaffolds, thiazolopyridinone urea
9 (scaffold A), thiazolopyridine urea (scaffold B) and benzothiazole urea (scaffold C) of
10 the molecules are depicted in Figure 1. These derivatives shared the thiazole urea core
11 structure and the inhibitory activities against GyrB and mycobacterial cell of these
12 inhibitors were measured by *M. smegmatis* GyrB ATPase assay and *M. tuberculosis*
13 H37Rv cell on MABA assay in the same laboratory. The IC₅₀ and MIC values of the
14 collected thiazole urea derivatives are in the range from 0.5 to 217 nM and 0.06 to 21
15 μM. Three-dimensional coordinate of inhibitors was downloaded from ChEMBL
16 database and used as initial coordinate for structure optimizations. M062X/6-31G* basis
17 set implemented in Gaussian 09 program was applied for structural optimizations. The
18 biological activities of thiazole urea core derivatives were converted into log(1/IC₅₀) and
19 log(1/MIC) for GyrB inhibitory activity and anti-mycobacterial activity to reduce the
20 range of biological activities, which serves as dependent variable for QSAR study.
21 Thiazole urea core derivatives were classified as two datasets, training set for QSAR
22 model construction and test set for validations of QSAR model. 9 compounds of test set
23 were selected by consideration of the structural diversity and the biological activity range
24 of thiazole urea derivatives.

25

26 **[Figure 1.]**

27 **[Table 1.]**

28 *HQSAR studies*

29 HQSAR approach [32] was performed using SYBYL X-2.0 [33] to investigate
30 the structural requirement for improving the biological activities. 55 GyrB inhibitors were

1 classified into two main classes, training set (46 compounds, 84 %) and test set (9
2 compounds, 16 %). For HQSAR analysis, four molecular fragments, atom (A), bond (B),
3 component (C) and donor and acceptor (DA) were selected as the independent molecular
4 descriptors and biological activities were used as dependent variable for HQSAR model
5 contractions. To develop robust HQSAR models, numerous models with various
6 combinations of the fragment-distinction properties were constructed. Partial least square
7 (PLS) was used to contrast the models of relationship of HQSAR descriptors and
8 biological activity ($\log(1/IC_{50})$ or $\log(1/MIC)$). The best HQSAR model was selected
9 depending based on leave-one-out cross-validation (q^2) higher than 0.6, lower standard
10 error (SE) value and the best cross-validated r^2 .

11 *3D-QSAR studies*

12 CoMFA [34,35] and CoMSIA [36] approaches were performed using SYBYL X-
13 2.0. The data set to set up CoMFA and CoMSIA model is the same set used in HQSAR
14 approach. The pharmacophore alignment module with the Genetic Algorithm with Linear
15 Assignment for Hypermolecular Alignment of Datasets (GALAHAD) was used as
16 molecular alignment tool for thiazole urea derivatives. GALAHAD is a developed
17 program that uses genetic algorithm (GA) to generate pharmacophore hypotheses by
18 ranging of energy profile, specificity value, and Pareto ranking [37-40] based on shared
19 pharmacophoric and pharmacosteric features. The best docking conformation of the most
20 active compound, compound **51** was used as template coordinate for molecular alignment
21 for 3D-QSAR CoMFA and CoMSIA studies. GALAHAD was run for 20 maximum
22 iterations with a population size of 40 with 20 pharmacophore models creations. The
23 conformation that aligned to best pharmacophore model was selected. CoMFA
24 descriptors, steric (S) and electrostatic (E) were calculated in standard settings with the
25 energy cut-off values of 30 kcal/mol. The CoMSIA similar indices descriptors including
26 steric (S) and electrostatic (E), hydrophobic (H), hydrogen-bond donor (D) and hydrogen-
27 bond acceptor (A) fields with attenuation factor α value of 0.3 and a grid spacing of 2 Å
28 were calculated. After descriptor generation, PLS methodology was performed to find the
29 correlation between dependent variables ($\log(1/IC_{50})$ or $\log(1/MIC)$) and independent
30 variable (CoMFA and CoMSIA descriptors). The q^2 of model higher than 0.6 with highest
31 r^2 were used to evaluate the predictive ability of 3D-QSAR models and used as the criteria
32 to accept the best and reliable 3D-QSAR model.

1 ***Molecular docking calculations***

2 GyrB ATPase domain of *Mycobacterium smegmatis* (*M. smegmatis*) complexed
3 with RWX (2-[(3*S*,4*R*)-4-[(3-bromanyl-4-chloranyl-5-methyl-1*H*-pyrrol-2-yl)carbonyl
4 amino] -3-methoxy-piperidin-1-yl]-4-(2-methyl-1,2,4-triazol-3-yl)-1,3-thiazole-5-
5 carboxylic acid) (PDB code 4BAE) was downloaded from protein databank and was used
6 as receptor coordinate for molecular docking [22]. Molecular docking was employed
7 using Autodock 2.4 program. The docking parameter was validated by docking of RWX
8 into the binding site. RWX ligand was used as centre of grid box (size 42×42×42 point)
9 with 0.375 Å spacing. The defeat docking parameter with 300 run of Lamarckian Genetic
10 Algorithm (LGA) were applied [41]. The RMSD between docked and x-ray conformation
11 lower than 1 Å (0.72±0.06, n=3) was used as criteria for acceptable docking parameters.
12 All selected thiazole urea core compounds for MD simulations were docked into the GyrB
13 ATPase binding site using the same docking parameter of RWX compound. The lowest
14 docking energy conformation was selected as the binding mode of thiazole urea cores in
15 the active site of GyrB ATPase.

16 ***MD simulations***

17 The binding mode and binding interactions of selected derivatives were discussed
18 in the original paper of thiazole urea derivatives. However, these results were obtained
19 from flexible-rigid docking calculations [28]. To obtain reliability and accuracy of the
20 binding mode and binding interactions of thiazole derivative in GyrB ATPase binding
21 site in the solvation system and full flexibility of GyrB ATPase, six thiazole urea core
22 derivatives covering the range of the most active to low active compounds were selected
23 for MD simulations. Compound **51** is represented as the most active compound with IC₅₀
24 of 0.5 nM, whereas compounds **55** with IC₅₀ value of 160 nM is representative compound
25 possessing weak inhibitory activities against GyrB. Moreover, compounds **25**, **26**, **30** and
26 **35** are represented as moderate compounds. The IC₅₀ values of moderate compounds are
27 in range of 3.7 to 88 nM. MD simulations using AMBER16 package [42] was employed
28 to elucidate the binding model and their crucial binding interactions in GyrB ATPase
29 domain. The initial structure of GyrB ATPase-thiazole urea core complexes were
30 obtained from flexible-rigid docking calculations using Autodock 4.2 as described in
31 molecular docking calculations section above. FF14SB [43] and general amber force field
32 (GAFF) [44] were applied as parameter for GyrB ATPase and thiazole urea core ligands,

1 respectively. All missing hydrogen atoms of GyrB ATPase were added using the LEaP
2 module. The restrained electrostatic potential (RESP) partial charges calculated at HF/6-
3 31G* [45] were assigned as atomic charges of thiazole urea core ligands by the
4 antechamber module implemented in the AMBER16 package. Each complex structure
5 was solvated by cubic box of TIP3P [46] water molecules extending up to 10 Å from each
6 solute species. Sodium cations (Na⁺) were added to neutralize the charge of each system.
7 To relax the bad steric interaction of water molecules and ions, the systems were first
8 minimized with atomic positions of all solute species restraint (using a force constant of
9 500 kcal mol⁻¹ Å⁻²) with 2,500 steps of steepest descents followed by 20,000 steps of
10 conjugated gradient. Non-bonded cut-off was set to 8 Å. Then, the system was gradually
11 warmed up from 0 to 300 K in the first 20 ps followed by maintaining the temperature at
12 300 K in the last 10 ps with 2 fs time simulation steps with a restraint weight of 2 kcal
13 mol⁻¹ Å⁻². After minimization and heating step, the position-restrained dynamics
14 simulations were applied to relax the positions of the solvent molecules for 70 ps at 300
15 K under an isobaric condition. Finally, 100 ns of MD simulations were performed for
16 each system without any restraints. The long-range electrostatic interactions were treated
17 by the Particle Mesh Ewald method (PME) [47] and the cut-off distance for the long-
18 range van der Waals interaction was set to 8 Å. To constrain the bond lengths of hydrogen
19 atoms attached to heteroatoms, the SHAKE method was applied [48].

20 ***Binding free energy calculations***

21 Two binding free energy calculation approaches, MM-GBSA [49, 50] and
22 waterswap calculations using Sire program [51, 52] were applied to estimate the binding
23 affinity of GyrB ATPase-thiazole urea core inhibitor complexed. For MM-GBSA, 4,000
24 snapshots during last 40 ns of MD simulations (after reached the equilibrium state) were
25 collected for the binding free energy calculations. Whereas, the waterswap calculation
26 approach used the final coordinate (100 ns of simulations) as initial structure for binding
27 free energy calculations.

28 ***Cluster analysis***

29 Cluster analysis was performed to determine the structure populations from MD
30 simulations, structure from last 40 ns of MD simulations were collected for clustering
31 analysis using cpptraj module [53] with average linkage. Distance cut-off for forming

1 cluster was set at 1.5 Å. The average structure from the highest structure populations was
2 selected for binding interaction analysis of thiazole urea cores in GyrB ATPase binding
3 site.

4 *Hydrogen bond analysis*

5 The percentage and the number of hydrogen bond (H-bond) occupations between
6 the selected thiazole urea core derivatives and the GyrB ATPase binding residues were
7 identified according to the subsequent criteria: (i) the distance between hydrogen-bond
8 donors (D) and hydrogen-bond acceptor (A) atoms ≤ 3.5 Å; and (ii) the D–H–A angle
9 ≥ 150 by cpptraj module of AMBER16 to detect all hydrogen bonds during last 40 ns of
10 MD simulations [53, 54].

11 **Results and Discussion**

12 *QSAR models*

13 The highest predictive ability for each developed HQSAR, CoMFA and CoMSIA
14 models was shown in Table 2 and 3, respectively. The best HQSAR-IC₅₀ model was
15 obtained with q^2 and r^2 values of 0.62 and 0.91, respectively. For the best HQSAR-MIC
16 model, q^2 and r^2 values were 0.60 and 0.90, respectively. The best model for HQSAR-
17 IC₅₀ and HQSAR-MIC contained three and four molecular fragment types which shared
18 two combination fragment types, donor and acceptor features (DA) and connections (C).
19 Only atoms (A) and bonds (B) were different combination to IC₅₀ HQSAR and MIC
20 HQSAR models, respectively. For 3D-QSAR model, only IC₅₀ CoMSIA model including
21 steric, electrostatic, hydrophobic and hydrogen donor fields was obtained with reliable q^2
22 value of 0.62 and r^2 of 0.98. The contribution of steric, electrostatic, hydrophobic and
23 hydrogen donor fields is 15%, 33%, 27% and 25%, respectively, indicating that the
24 electrostatic field shows greatest influence on the activity of thiazole derivatives against
25 GyrB inhibitory activity. Predicted biological activity of training set of IC₅₀ CoMSIA,
26 IC₅₀ HQSAR and MIC HQSAR models were predicted and summarized in Table 4. To
27 access the predictive abilities of each models, IC₅₀ and MIC values of the test set were
28 predicted as concluded in Table 4. The predicted activities of the training set are close to
29 the experimental activities with highest deviation values of 0.25, 0.43 and 0.69 logarithm
30 unit for IC₅₀ CoMSIA, IC₅₀ HQSAR and MIC HQSAR models, respectively. In addition,

1 deviation values between experimental and predicted activity of test set for IC₅₀ CoMSIA,
2 IC₅₀ HQSAR and MIC HQSAR models are 0.40, 0.40 and 0.44 (lower than one logarithm
3 unit) indicated that the QSAR models obtained from this work can be utilized to predict
4 the biological activity of newly design thiazole urea core derivatives. The experimental
5 and predicted activities of the IC₅₀ CoMSIA, IC₅₀ HQSAR and MIC HQSAR models
6 reveal a linear relationship (Figure 2).

7 [Table 2.]

8 [Table 3.]

9 [Table 4.]

10 [Figure 2.]

11 *HQSAR atomic contribution and molecular fragment analysis*

12 Molecular fragments of thiazole urea core derivatives which contribute directly to
13 biological activities of GyrB inhibition (IC₅₀) and mycobacterial cell inhibition (MIC)
14 can be visualized through HQSAR contribution maps. The HQSAR colour coding
15 demonstrates the atomic contributions of the compounds with regards to biological
16 activity. Green and yellow atomic contribution demonstrate a favourable contribution or
17 positive contribution with regards to biological activity, whereas red, red-orange and
18 orange indicate an unfavourable or negative contribution. White suggests an intermediate
19 contribution of the atoms towards inhibitory activity. The atomic distributions of highest
20 active compound **51**, moderate active compound **37** and low active compound **4** with IC₅₀
21 HQSAR and MIC HQSAR were exposed in Figure 3. For the IC₅₀ HQSAR model, the
22 highest active compound **51** and moderate active compound **37** exhibited the important
23 green and yellow fragments. In contrast, the lowest active compound (compound **4**) only
24 showed the bad fragments, orange and red fragments. The colour code labelling of MIC
25 HQSAR model reveals that thiazole urea core is crucial for inhibitory activity responsible
26 for GyrB enzyme and mycobacterial cell. R₂ and R₃ are positively favourable for anti-
27 mycobacterial activity as displayed in compound **51** (the highest active compound) and

1 compound **37** (moderate active compound). The low active compound **4** were labelled by
2 orange and red colour labelling. These results demonstrated that thiazole urea cores is key
3 fragment for favorable to high potency on IC₅₀ and MIC. In addition, R₂ and R₃
4 substituents were favorable to improv the anti-mycobacterial activity.

5 **[Figure 3.]**

6 **[Figure 4.]**

7 *CoMSIA contour maps*

8 The structural requirement to improve GyrB inhibitory activity were derived from
9 CoMSIA contour maps using the highest predictive ability IC₅₀ CoMSIA model as
10 displayed in Figure 5. The steric contour map was used to discriminate the steric structural
11 requirement. Green and yellow contours were steric favourable and steric unfavourable,
12 respectively. The electrostatic contour map was used to describe the effect of charge on
13 the structural requirement of thizaole derivatives. Red and blue contour represent the
14 negative charge and positive charge favourable, respectively. Magenta and white contour
15 of CoMSIA hydrophobic contour map present the hydrophobic and hydrophilic
16 properties favourable. The hydrogen bond donor and hydrogen bond favourable were
17 suggested by cyan and purple contour maps, respectively. Cyan contour map located very
18 closed to NH of urea fragment of thiazole urea core derivative indicate that hydrogen
19 bond donor property of this fragment was required to enhance the biological activity. All
20 data set compounds in this work contained this urea fragment. This is confirmed that urea
21 part was crucial for biological activity of thiazole urea core derivatives. At R₁ position,
22 there is only one small yellow contour appeared. Therefore, small substituent or low steric
23 hindrance substituent was required to improve the GyrB inhibitory activity. For example,
24 compound **21** and compound **22** contained allyl and ethyl substituent of thiazole urea core
25 scaffold A, respectively. The inhibitory activity (IC₅₀) of compound **21** was 50 nM that
26 showed the slightly higher inhibitory activity than compound **22** with IC₅₀ value of 40
27 nM. Compound **27** and **28** that represented as member of thiazole urea core scaffold B
28 were presented with allyl and ethyl substituents on R₁ position. Allyl substituent of
29 compound **27** produced lower biological activity than ethyl substituent of compound **28**
30 with the IC₅₀ of 46 nM and 25 nM for compound **27** and **28**, respectively. At R₂ position,
31 the green, red and white contours were displayed demonstrate that steric with negative

1 charge and hydrophilic properties were required for improving the biological activity of
2 thiazole urea core derivatives. For the steric effect on R₂ substituent, compounds **7**, **9**, **11**,
3 **14** and **15** showed difference biological activity against GyrB because of substituent size
4 of R₂ position. The increasing size of 3-fluoro-pyrimidinyl (compound **7**), 3-methoxy-
5 pyrimidinyl (compound **9**), 3-cyano-pyrimidinyl (compound **11**) and 1-alkyl-2(1*H*)-
6 pyridinonyl (compound **14** and **15**) confirmed that the biological activity of thiazole urea
7 core scaffold A (thiazolopyridinone) were increased for 10 nM, 6 nM, 4 nM, 5 nM and
8 2.5 nM for compounds **7**, **9**, **11**, **14** and **15**, respectively. The biological activity of
9 compounds **44**, **45** and **46** (thiazole urea core scaffold B) demonstrate that increasing of
10 substitution on 3th position of pyridinyl substituent R₂ enhanced the IC₅₀ values of 12
11 nM, 10 nM and 4 nM for compounds **44**, **45** and **46**, respectively. In addition, increasing
12 size of aromatic ring of R₂ substituent of thiazole urea core scaffold B were improved the
13 biological activity as exemplified in compounds **46**, **47** and **51**. Compound **47** containing
14 1-methylpyrazole substituent at R₂ position showed the biological activity lower than
15 compound **48** that contained 1-methyl-2(1*H*)-pyridinonyl substituent with IC₅₀ values of
16 10 nM and 1 nM for compounds **47** and **48**, respectively. In addition, compound **51**
17 containing larger substituent size on 2(1*H*)-pyridinonyl than compound **47** showed the
18 potency higher with the value of 0.5 nM and 1 nM, respectively. As considered with the
19 effect of electrostatic property on R₂ substituent, compounds **38**, **39**, **43**, **44** and **48** were
20 exemplified. Replacing H atom on pyridinyl ring of R₂ substituent of compound **38** by
21 high electronegativity fluorine atom (compound **39**) or CN group (compounds **43** and **44**)
22 were considered. The biological activity of compounds **39** and **43** were increased as
23 compared to compound **38** with the IC₅₀ of 90 nM, 7 nM, 14 nM and 12 nM for
24 compounds **38**, **39**, **43** and **44**, respectively. Adding an oxygen carbonyl on R₂ substituent,
25 the biological activity of thiazole urea core derivative was increased as depicted by
26 compounds **38** and **48**. Pyridinyl substituent on compound **38** produced low biological
27 activity than 1-methyl-2(1*H*)-pyridinonyl substituent on compound **48**. The effect of
28 hydrophobic property and hydrophilic properties of R₂ position on the biological activity
29 of thiazole urea core derivative was discriminated by compounds **6** and **18** in scaffold A.
30 Compound **6** showed the inhibitory activity higher than **18** due to more hydrophilic
31 favourable of pyrimidine of compound **6** as compared to pyridine ring of compound **18**.
32 Compounds **48-50** were used to exemplify the effect of hydrophilic property of R₂
33 position on thiazole urea core scaffold B derivatives. The increasing hydrophobic
34 property of compounds **49** and **50** effected to lower inhibitory activity than compound **48**.

1 At R₃ position of scaffold B, this position required the steric substituent to improve the
2 biological activity. For example, compound **27** showed high potency than compound **26**
3 due to the steric substituent. In addition, compound **30** contained heterocyclic aliphatic
4 substituent which they showed the potency higher than compound **34** (linear aliphatic
5 chain). The hydrophobic substituent improved the biological activity of thiazole urea core
6 scaffold B. For example, compounds **30**, **31** and **32** which contained different R₃
7 substituent showed different inhibitory activities. Compound **30** with 3-
8 methyltetrahydrofuran displayed the potency higher than compounds **31** and **32** that
9 contained tetrahydropyran and tetrahydrofuran substituents, respectively.

10
11 **[Figure 5.]**

12 *MD simulations*

13 The root-mean square deviations (RMSD) over the simulations time of solute
14 species, GyrB ATPase and selected ligands were calculated and plotted as shown in
15 Figure 6. MD simulations systems of GyrB ATPase and selected ligands reach the
16 equilibrium state after 40 ns, 50 ns, 30 ns, 60 ns, 10 ns and 10 ns for compounds **25**, **26**,
17 **30**, **35**, **51** and **55**, respectively. Therefore, the MD snapshots after 60 ns of the simulations
18 time were selected for binding free energy calculations and structural analysis.

19
20 **[Figure 6.]**

21
22 The binding free energy of thiazole urea cores complexed with GyrB ATPase with
23 two calculation methods were summarised in Table 4 and Figure 7. Both binding free
24 calculation methods were corrected order of active compounds. The correlation (R²)
25 between experimental binding free energy and calculated binding free energy from MM-
26 GBSA and waterswap are 0.52 and 0.85, respectively. In addition, waterswap calculations
27 showed higher correlation than MM-GBSA approach. These results indicated that the
28 binding mode of thiazole urea core derivatives are corrected based on the correlation
29 between experimental and calculated binding free energy approved. [The obtained results](#)

1 from these binding energy calculations demonstrated that the conformation obtained from
2 MD simulations can produced the corrected order of binding free energy and GyrB
3 inhibitory activity. Therefore, the finding binding mode from MD simulations is reliable
4 for investigation of the binding mode and crucial interactions for binding of thiazole urea
5 core derivatives in the GyrB ATPase domain.

6
7 [Table 4.]

8 [Figure 7.]

9 *The binding interactions of thiazole urea core derivatives in GyrB ATPase*
10 *domain*

11 The binding mode of thiazole urea core derivatives was examined to investigate
12 the key binding interactions in GyrB ATPase binding site. The binding interactions of
13 the highest active compound **51** was analysed and showed in Figure 8. Compound **51**
14 formed two hydrogen bond interactions with Asp79 and Arg141. A NH of urea fragment
15 of thiazole urea core compound **51** interacted with oxygen atoms of Asp79 sidechain.
16 Hydrogen atom of Asn52 point to thiazole aromatic ring of inhibitor and formed sigma-
17 pi interaction. Glu56 sidechain closed to thiazole ring and formed van der Waals
18 interaction. Ethyl R₁ substituent interacted with hydrophobic interaction with Val49,
19 Ala53, Val65, Val77, Thr169 and Ile171 sidechain. An oxygen carbonyl of R₂ substituent
20 from hydrogen bond interaction with NH sidechain of Arg141. Cation-pi was obtained
21 between guanidinium cation sidechain of Arg82 with aromatic ring of R₂ substituent of
22 compound **51**. In addition, hydrophobic interactions of R₂ substituent of this compound
23 **51** with Arg82, Gly83 and Pro85 were achieved. For R₃ substituent of compound **51**, this
24 substituent contacted with Ile84, Pro85, Thr95, Val99, Leu120 and Val123 sidechains by
25 hydrophobic interactions. These results were supported by the interaction energy using
26 MM-GBSA calculation and hydrogen bond analysis as shown in Figure 9 and Figure 10.
27 Figure 9e showed the binding interactions energy of compound **51**. Large energy
28 contribution was observed from the interaction of compound **51** with Asp79 with -12.0
29 kcal/mol. In addition, the interaction energy of Arg141 with an oxygen of carbonyl group
30 support the strong binding affinity of compound **51** with -8.1 kcal/mol. For all selected

1 compounds, the binding interaction energy profiles were similar to the energy profile of
2 compound **51** due to hydrogen bond interaction of nitrogen atom on pyridinyl substituent
3 with Arg141, except compound **25**. Compound **25** formed additional hydrogen bond
4 interaction between an oxygen carbonyl of urea core with NH sidechain of Asn52. Based
5 on six selected compounds for MD simulation in this study, we found that three residues,
6 Asn52, Asp79 and Arg141 of GyrB ATPase formed hydrogen interaction with thiazole
7 urea core derivatives as shown in Figure 10. An oxygen atom of Asp79 sidechain act as
8 hydrogen bond acceptor to bind with NH of urea of thiazole urea core derivatives along
9 the hydrogen bond interaction with % hydrogen bond occupation higher than 50 %. This
10 result suggested that hydrogen bond interactions were crucial interaction for binding with
11 GyrB ATPase domain of thiazole urea core derivative via the hydrogen bond interactions
12 with Asp79. In addition, hydrogen bond interaction with Arg141 of R₂ substituents
13 improved the biological activity of thiazole urea core derivatives against GyrB as shown
14 in Figure 10. As compared to the docking results from original paper, the crucial
15 interactions in ATPase binding site were similar. Asp79 interacted with NH of urea core
16 via hydrogen bond interactions. Hydrogen bond interactions of an oxygen carbonyl and
17 NH of Arg141 sidechain was also reported [28]. However, there are no hydrogen bond
18 linker interactions water molecules by of nitrogen atom of thiazole ring with oxygen
19 carbonyl of Asp79 sidechain and an oxygen carbonyl of urea core with NH of Asn52
20 based on MD simulations and waterswap calculations in the present study. Therefore,
21 water molecule doesn't affect to the binding interactions of thiazole urea derivatives in
22 ATPase binding site.

23

[Figure 8.]

24

[Figure 9.]

25

[Figure 10.]

26

27 *The key structural feature of thiazole derivatives for highly potent biological* 28 *activities*

29 In the present study, well-known QSAR approaches were carried out to
30 understand the key structural requirements of thiazole urea derivatives responsible to both
31 GyrB enzyme and mycobacterial cell. These finding provides the critical information to
32 rational design of new highly potent thiazole urea inhibitors. Based on the MD
33 simulations results, the quantitative information of binding mode and binding interactions

1 was obtained from the solvation system by high accuracy of calculation method. The
2 integrations of QSAR and MD simulations results provided the essential structural
3 features for rational design of new and highly potent inhibitors with specific to GyrB
4 ATPase binding site. The structural requirements and key interaction for binding of
5 thiazole urea core derivatives for good potency against both IC₅₀ and MIC derived from
6 QSAR models and MD simulations approaches were summarized in Figure 11. Based on
7 HQSAR, CoMSIA and MD simulations, the common structural features required for
8 inhibition of GyrB enzyme and mycobacterial cell are revealed. The results of HQSAR
9 based on two different biological activities, IC₅₀ and MIC, suggest that the thiazole urea
10 core was the key structure to obtain the inhibitory activities against both GyrB enzyme
11 and mycobacterial cell. Urea fragment structure of thiazole urea core derivatives was
12 crucial fragment for binding in GyrB ATPase binding pocket with hydrogen bond
13 interactions with Asp79. These results demonstrated that thiazole urea core should be
14 kept for good potency against both enzyme and bacterial cell. To improve the potencies,
15 small substituent at R₁ position was required to interact with hydrophobic side chain of
16 GyrB. A R₂ position, steric substituent like heterocyclic aromatic ring with hydrophilic
17 property and suitable position of negative charge were required to bind with Arg82,
18 Arg141 and hydrophobic residues via hydrogen bond interaction, cation-pi interaction
19 and hydrophobic interactions, respectively. For R₃ position, steric substituent with
20 hydrophobic property was required to enhance the inhibitory activities of thiazole urea
21 core derivatives. An extensive analysis of QSAR and MD simulations was very useful to
22 design new drug candidates against GyrB ATPase targets. In addition, QSAR models can
23 be an useful tool to guide further inhibitors design studies for the optimizations and
24 development of new thiazole ureas having improved GyrB ATPase binding affinity.
25 Considering the results obtained in the present study, the improvement of lead and
26 candidate of the DNA gyrase inhibitors status in a series of thiazole urea derivatives.

27

28

[Figure 11.]

29 *Rational design of novel thiazole urea derivatives*

30 Novel thiazole urea derivatives were designed based on our obtained results. The
31 R₂ and R₃ substituents were modified, whereas thiazole urea core and the ethyl R₁
32 substituent were kept as the general structure. Heterocyclic aromatic rings were added to

1 the R₂ position with the aim for forming the cation- π interaction with Arg82. Steric
2 substituents with hydrophobic property were introduced to the R₃ position. For designing
3 new DNA gyrase inhibitors, the physicochemical properties and pan assay interference
4 compounds (PAINS) violation were considered for the novel DNA gyrase inhibitors
5 using SwissADME prediction [55]. The HQSAR-IC₅₀ and HQSAR-MIC models were
6 used to predict the biological activities of novel thiazole urea derivatives. 1,200 novel
7 thiazole urea derivatives were designed based on the finding key structural features. In
8 general, the log(1/IC₅₀) and log(1/MIC) higher than 7.00 and 6.00 were required as potent
9 GyrB inhibitor of thiazole urea derivative [28]. Based on HQSAR-IC₅₀ and HQSAR-MIC
10 predictions, 407 thiazole urea derivatives were collected based on log(1/IC₅₀) and
11 log(1/MIC) prediction higher than 7.00 and 6.00, respectively. preADME [56] was
12 applied to predict the pharmacokinetic parameters of novel designed compounds as well
13 as the most active compound **51** as shown in Table 5. The most active compound **51**
14 displayed low blood-brain barrier (BBB) penetration and plasma protein binding (PPB)
15 with the values of 0.02 and 49.66%, respectively. Moderate value of MadinDarby Canine
16 Kidney (MDCK) cell models for oral drug absorption was obtained with the value of
17 4.64. High heterogeneous human epithelial colorectal adenocarcinoma cell lines (Caco2-
18 cell) and HIA were obtained with the values of 38.87 and 94.70, respectively. The BBB
19 values of designed thiazole urea derivatives higher than the most active compound **51**
20 (>0.02) were considered. 200 compounds (Table S1) display the BBB values higher than
21 the most active compound **51**. **D007** and **D063** showed the highest predicted log(1/IC₅₀)
22 and log(1/MIC) with the values of 8.40 and 6.51, respectively. Their structures drug like
23 properties and pharmacokinetic were summarized in Figure 12 and Table 5. The
24 pharmacokinetic properties of designed compounds were acceptable, except MDCK cell
25 level. Interestingly, PPB of novel designed compounds were higher than the most active
26 compound **51**. The binding modes of **D007** and **D063** were predicted using docking
27 calculations. The binding energies of compounds **D007** and **D063** are -9.66 and -7.97
28 kcal/mol, respectively indicating that these compounds are favourable for binding in
29 ATPase domain of GyrB. The predicted binding modes of compounds **D007** and **D063**
30 in ATPase binding pocket are shown in Figures 13a and 13b, respectively. NH of the urea
31 core structure interacts with the oxygen carboxylate of Asp79 sidechain by hydrogen
32 bond interactions. Cation- π interaction with Arg82 was found between the aromatic R₂
33 substituent of both compounds (**D007** and **D063**). In addition, the nitrogen atoms on
34 pyrimidine ring of **D007** and oxadiazole ring of **D063** form the hydrogen bond

1 interactions with Arg141. These results demonstrated that the novel designed compounds
2 can be proposed as new DNA gyrase inhibitors with good pharmacokinetic properties and
3 strongly bind with ATPase domain.

4
5 **[Figure 12]**

6 **[Table 5]**

7 **[Figure 13]**

8 **Conclusion**

9 The key structural features of thiazole urea core derivative responsible for high
10 potency against of GyrB and mycobacterial cell inhibition were successfully investigated
11 by HQSAR, CoMSIA and MD simulations. IC₅₀ HQSAR, MIC HQSAR and IC₅₀
12 CoMSIA models have high power to predict the activities of thiazole urea core
13 derivatives. The reliable binding modes, binding free energy, and binding interactions of
14 thiazole urea core derivatives in the GyrB ATPase binding pocket were obtained by MD
15 simulations. **Based on MD simulations, the crucial interactions of thiazole urea**
16 **derivatives were corresponded well to previously report from the original paper. In**
17 **contrast, water molecules were not stabilized the hydrogen interactions of thiazole urea**
18 **derivatives with amino acid residues surrounding their binding site.** The combination of
19 graphical interpretation of QSAR results and MD simulations provides a key insight into
20 the structural features needed to increase the IC₅₀ and MIC values of thiazole urea core
21 derivatives. Thiazole urea core and R₂ substituent were required to attaining favorable
22 IC₅₀ and MIC values, whereas the R₃ substituent is the key to enhance the potency against
23 IC₅₀. Therefore, the results obtained from this study should facilitate the further
24 modification of thiazole urea core derivatives for generating novel DNA gyrase inhibitors
25 with improved GyrB and mycobacterial cell inhibition potency. **Therefore, novel thiazole**
26 **urea derivatives with good predicted biological activities and pharmacokinetic properties**
27 **were proposed as potent DNA gyrase inhibitors.**

28 **Acknowledgements**

29 This research was supported by the Thailand Research Fund (MRG6180147 and
30 RSA5980057) and the Health Systems Research Institute (HSRI.60.083). This work has
31 been facilitated by the BrisSynBio Biosuite (UK Biotechnology and Biological Sciences

1 (BBSRC) and Engineering and Physical Sciences (EPSRC) Research Councils,
2 BB/L01386X/1) and the BBSRC ALERT14 equipment initiative (BB/M012107/1). AJM
3 and JS acknowledge funding from the BristolBridge antimicrobial resistance network
4 (EPSRC EP/M027546/1). We thank CCP-BioSim (grant number EP/M022609/1) for
5 funding. The University of Bristol are gratefully acknowledged for computational
6 resource supports of this research. Nakhon Phanom University, Ubon Ratchathani
7 University, NECTEC and University of Bristol are gratefully acknowledged for
8 supporting this research.

9 **References**

- 10 [1] https://www.who.int/tb/publications/global_report/GraphicExecutiveSummary.pdf?ua=1
- 11 [2] R. Dhiman and R. Singh, *Recent advances for identification of new scaffolds and drug*
12 *targets for Mycobacterium tuberculosis*, IUBMB Life. 70(9) (2004), pp. 905-916.
- 13 [3] A. Bahuguna and D.S. Rawat, *An overview of new antitubercular drugs, drug candidates,*
14 *and their targets*, Med. Res. Rev. (2019), <https://doi.org/10.1002/med.21602>.
- 15 [4] A.K. Saxena and A. Singh, *Mycobacterial tuberculosis Enzyme Targets and their*
16 *Inhibitors*, Curr Top Med Chem. 19 (2019), pp. 337-355.
- 17 [5] J.M., Blondeau, *Fluoroquinolones: Mechanism of action, classification, and development*
18 *of resistance*, Surv. Ophthalmol. 49 (2004), pp. S73-78.
- 19 [6] K. Mdluli and Z. Ma, *Mycobacterium tuberculosis DNA gyrase as a target for drug*
20 *discovery*, Infect. Disord. Drug. Targets. 7 (2007), pp. 159-168.
- 21 [7] A. Kashyap, P.K. Singh and O. Silakari, *Chemical classes targeting energy supplying*
22 *GyrB domain of Mycobacterium tuberculosis*, Tuberculosis (Edinb). 113 (2018), pp. 43-
23 54.
- 24 [8] K. Chaudhari, S. Surana, P. Jain and H.M. Patel, *Mycobacterium tuberculosis (MTB) GyrB*
25 *inhibitors: An attractive approach for developing novel drugs against TB*. Eur. J. Med.
26 Chem. 124 (2016), pp. 160-185.
- 27 [9] V. Nagaraja, A.A. Godbole, S.R. Henderson and A. Maxwell, *DNA topoisomerase I and*
28 *DNA gyrase as targets for TB therapy*, Drug Discov. Today. 22 (2017), pp. 510-518.
- 29 [10] K.J. Aldred, R.J. Kerns and N. Osheroff, *Mechanism of quinolone action and resistance*,
30 Biochemistry. 53 (2014), pp. 1565-1574.

- 1 [11] T. Khan, K. Sankhe, V. Suvarna, A. Sherje, K. Patel and B. Dravyakar, *DNA gyrase*
2 *inhibitors: Progress and synthesis of potent compounds as antibacterial agents*, Biomed.
3 Pharmacother. 103 (2018), pp. 923-938.
- 4 [12] J.H. Morais Cabral, A.P. Jackson, C.V. Smith, N. Shikotra, A. Maxwell and R.C.
5 Liddington, *Crystal structure of the breakage-reunion domain of DNA gyrase*, Nature. 388
6 (1997), pp. 903-906.
- 7 [13] B.D. Bax, P.F. Chan, D.S. Eggleston, A. Fosberry, D.R. Gentry, F. Gorrec, I. Giordano,
8 M.M. Hann, A. Hennessy, M. Hibbs, J. Huang, E. Jones, J. Jones, K.K. Brown, C.J.
9 Lewis, E.W. May, M.R. Saunders, O. Singh, C.E. Spitzfaden, C. Shen, A. Shillings, A.J.
10 Theobald, A. Wohlkonig, N.D. Pearson and M.N. Gwynn, *Type IIA topoisomerase*
11 *inhibition by a new class of antibacterial agents*, *Type IIA topoisomerase inhibition by a*
12 *new class of antibacterial agents*, Nature. 466 (2010), pp.935-940.
- 13 [14] F. Collin, S. Karkare and A. Maxwell, *Exploiting bacterial DNA gyrase as a drug target:*
14 *current state and perspectives*, Appl. Microbiol. Biotechnol. 92 (2011), pp. 479-497.
- 15 [15] A. Agrawal, M. Roué, C. Spitzfaden, S. Petrella, A. Aubry, M. Hann, B. Bax and C.
16 Mayer, *Mycobacterium tuberculosis DNA gyrase ATPase domain structures suggest a*
17 *dissociative mechanism that explains how ATP hydrolysis is coupled to domain motion*,
18 Biochem. J. 456 (2013), pp. 263-273.
- 19 [16] E. Avalos, D. Catanzaro, A. Catanzaro, T. Ganiats, S. Brodine, J. Alcaraz and T. Rodwell,
20 *Frequency and geographic distribution of gyrA and gyrB mutations associated with*
21 *fluoroquinolone resistance in clinical Mycobacterium tuberculosis isolates: a systematic*
22 *review*, PLoS One. 10 (2015), pp. e0120470.
- 23 [17] A. Von Groll, A. Martin, P. Jureen, S. Hoffner, P. Vandamme, F. Portaels, P.C. Palomino
24 and P.A. da Silva, *Fluoroquinolone resistance in Mycobacterium tuberculosis and*
25 *mutations in gyrA and gyrB*, Antimicrob. Agents Chemother. 53 (2009), pp. 4498-4500.
- 26 [18] A.S. Ginsburg, J.H. Grosset and W.R. Bishai, *Fluoroquinolones, tuberculosis, and*
27 *resistance*, Lancet Infect. Dis. 3 (2003), pp. 432-442.

- 1 [19] F. Maruri, T.R. Sterling, A.W. Kaiga, A. Blackman, Y.F. van der Heijden, C. Mayer, E.
2 Cambau and A. Aubry, *A systematic review of gyrase mutations associated with*
3 *fluoroquinolone-resistant Mycobacterium tuberculosis and a proposed gyrase numbering*
4 *system, J. Antimicrob. Chemother.* 67 (2012), pp. 819-831.
- 5 [20] B. Medapi, P. Suryadevara, J. Renuka, J.P. Sridevi, P. Yogeeswari and D. Sriram, *4-*
6 *Aminoquinoline derivatives as novel Mycobacterium tuberculosis GyrB inhibitors:*
7 *Structural optimization, synthesis and biological evaluation, Eur. J. Med. Chem.* 103
8 (2015), pp. 1-16.
- 9 [21] V.U. Jeankumar, J. Renuka, P. Santosh, V. Soni, J.P. Sridevi, P. Suryadevara, P.
10 Yogeeswari and D. Sriram, *Thiazole-aminopiperidine hybrid analogues: design and*
11 *synthesis of novel Mycobacterium tuberculosis GyrB inhibitors, Eur. J. Med. Chem.* 70
12 (2013), pp. 143-153.
- 13 [22] S.H. P, S. Solapure, K. Mukherjee, V. Nandi, D. Waterson, R. Shandil, M. Balganes, S.
14 V.K. Sambandamurthy, A.K. Raichurkar, A. Deshpande, A. Ghosh, D. Awasthy, G.
15 Shanbhag, G. Sheikh, H. McMiken, J. Puttur, J. Reddy, J. Werngren, J. Read, R.M. Kumar
16 M, M. Chinnapattu, P. Madhavapeddi, P. Manjrekar, R. Basu, S. Gaonka, S. Sharma, S.
17 Hoffner, V. Humnabadkar, V. Subbulakshmi and V. Panduga, *Optimization of*
18 *pyrrolamides as mycobacterial GyrB ATPase inhibitors: structure-activity relationship*
19 *and in vivo efficacy in a mouse model of tuberculosis, Antimicrob. Agents Chemother.* 58
20 (2014), pp. 61-70.
- 21 [23] S. Saxena, G. Samala, J. Renuka, Y.P. Sridevi, P. Yogeeswari and D. Sriram,
22 *Development of 2-amino-5-phenylthiophene-3-carboxamide derivatives as novel inhibitors*
23 *of Mycobacterium tuberculosis DNA GyrB domain, Bioorg. Med. Chem.* 23 (2015), pp.
24 1402-1412.
- 25 [24] B. Medapi, J. Renuka, S. Saxena, J.P. Sridevi, R. Medishetti, P. Kulkarni, P. Yogeeswari
26 and D. Sriram, *Design and synthesis of novel quinoline-aminopiperidine hybrid analogues*
27 *as Mycobacterium tuberculosis DNA gyraseB inhibitors, Bioorg. Med. Chem.* 23 (2015),
28 pp. 2062-2078.

- 1 [25] J. Renuka, K.I. Reddy, K. Srihari, V.U. Jeankumar, M. Shravan, J.P. Sridevi, P.
2 Yogeeswari, K.S. Babu and D. Sriram D, *Design, synthesis, biological evaluation of*
3 *substituted benzofurans as DNA gyraseB inhibitors of Mycobacterium tuberculosis,*
4 *Bioorg. Med. Chem.* 22 (2014), pp. 4924-4934.
- 5 [26] K.I. Reddy, K. Srihari, J. Renuka, K.S. Sree, A. Chuppala, V.U. Jeankumar, J.P. Sridevi,
6 K.S. Babu, P. Yogeeswari and D. Sriram, *An efficient synthesis and biological screening*
7 *of benzofuran and benzo[d]isothiazole derivatives for Mycobacterium tuberculosis DNA*
8 *GyrB inhibition,* *Bioorg. Med. Chem.* 22 (2014), pp. 6552-6563.
- 9 [27] R.R. Kale, M.G. Kale, D. Waterson, A. Raichurkar, S.P. Hameed, M.R. Manjunatha, B.K.
10 Kishore Reddy, K. Malolanarasimhan, V. Shinde, K. Koushik, L.K. Jena, S. Menasinakai,
11 V. Humnabadkar, P. Madhavapeddi, H. Basavarajappa, S. Sharma, R. Nandishaiah, K.N.
12 Mahesh Kumar, S. Ganguly, V. Ahuja, S. Gaonkar, C.N. Naveen Kumar, D. Ogg D, P.A.
13 Boriack-Sjodin, V.K. Sambandamurthy, S.M. de Sousa and S.R. Ghorpade,
14 *Thiazolopyridone ureas as DNA gyrase B inhibitors: Optimization of antitubercular*
15 *activity and efficacy,* *Bioorg. Med. Chem. Lett.* 24 (2014), pp. 870-879.
- 16 [28] M.G. Kale, A. Raichurkar, S.H. P, D. Waterson, D. McKinney, M.R. Manjunatha, U.
17 Kranthi, K. Koushik, Lk. Jena, V. Shinde, S. Rudrapatna, S. Barde, V. Humnabadkar, P.
18 Madhavapeddi, H. Basavarajappa, A. Ghosh, V.K. Ramya, S. Guptha, S. Sharma, P.
19 Vachaspati, K.N. Kumar, J. Giridhar, J. Reddy, V. Panduga, S. Ganguly, V. Ahuja, S.
20 Gaonkar, C.N. Kumar, D. Ogg, J.A. Tucker, P.A. Boriack-Sjodin, S.M. de Sousa, V.K.
21 Sambandamurthy and S.R. Ghorpade, *Thiazolopyridine ureas as novel antitubercular*
22 *agents acting through inhibition of DNA gyrase B,* *J. Med. Chem.* 56 (2013), pp. 8834-
23 8848.
- 24 [29] Dipiksh, M. Salman and S. Nandi, *QSAR and pharmacophore modeling of anti-tubercular*
25 *6-Fluoroquinolone compounds utilizing calculated structural descriptors,* *Med. Chem.*
26 *Res.* 26 (2017), pp. 1903-1914.
- 27 [30] N. Minovski, M. Vracko and T. Šolmajer, *Quantitative structure–activity relationship*
28 *study of antitubercular fluoroquinolones,* *Mol. Divers.* 15 (2011), pp. 417-426.

- 1 [31] S. Nandi, S. Ahmed and A.K. Saxena, *Combinatorial design and virtual screening of*
2 *potent anti-tubercular fluoroquinolone and isothiazoloquinolone compounds utilizing*
3 *QSAR and pharmacophore modelling*, SAR QSAR Environ. Res. 29 (2018), pp. 151-170.
- 4 [32] TRIPOS Associates, Inc, Sybyl-X Molecular Modeling Software Packages, St. Louis, MO,
5 498 USA, 2012.
- 6 [33] SYBYL-X 2.0. Tripos Inc., St. Louis, MO, 2015.
- 7 [34] R.D. Cramer, D.E. Patterson and J.D. Bunce, *Comparative molecular field analysis*
8 *(CoMFA). 1. Effect of shape on binding of steroids to carrier proteins*, J. Am. Chem. Soc.
9 110 (1988), pp. 5959-5967.
- 10 [35] M. Clark, R.D. Cramer III, D.M. Jones, D.E. Patterson and P.E. Simeroth, *Comparative*
11 *molecular field analysis (CoMFA). 2. Toward its use with 3D-structural databases*,
12 *Tetrahedron Comput. Methodol.* 3 (1990), pp. 47-59.
- 13 [36] G. Klebe, U. Abraham and T. Mietzner, *Molecular similarity indices in a comparative*
14 *analysis (CoMSIA) of drug molecules to correlate and predict their biological activity*, J.
15 *Med. Chem.* 37 (1994), pp. 4130-4146.
- 16 [37] N.J. Richmond., CA. Abrams, P.R. Wolohan, E. Abrahamian, P. Willett and R.D. Clark,
17 *GALAHAD: 1. pharmacophore identification by hypermolecular alignment of ligands in*
18 *3D*, J. Comput. Aided. Mol. Des. 20 (2006), pp. 567-587.
- 19 [38] Y. Xiang, Z. Hou and Z. Zhang, *Pharmacophore and QSAR studies to design novel*
20 *histone deacetylase 2 inhibitors*, Chem. Biol. Drug Des. 79 (2012), pp. 760-770.
- 21 [39] R. Uddin, M. U. Lodhi and Z. Ul-Haq, *Combined pharmacophore and 3D-QSAR study on*
22 *a series of Staphylococcus aureus Sortase A inhibitors*, Chem. Biol. Drug Des. 80 (2012),
23 pp. 300-314.
- 24 [40] K.C. Weber, L.B. Salum, K.M. Honório, A.D. Andricopulo and A.B. da Silva,
25 *Pharmacophore-based 3D QSAR studies on a series of high affinity 5-HT_{1A} receptor*
26 *ligands*, Eur. J. Med. Chem. 45 (2010), pp. 1508-1514.
- 27 [41] R. Huey, G.M. Morris, A.J. Olson and D.S. Goodsell, *A semiempirical free energy force*
28 *field with charge-based desolvation*, J. Comput. Chem. 28 (2007), pp. 1145-1152.
- 29 [42] P.A.K. D.A. Case, R.M. Betz, W. Botello-Smith, D.S. Cerutti, T.E. Cheatham III, T.A.
30 Darden, R.E. Duke, T.J. Giese, H. Gohlke, A.W. Goetz, N. Homeyer, S. Izadi, P.

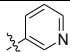
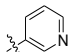
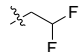
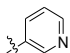
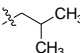
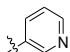
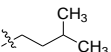
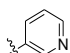
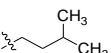
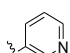
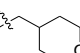
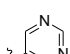
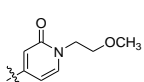
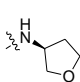
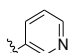
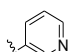
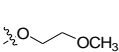
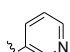
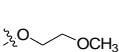
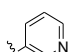
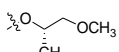
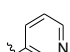
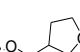
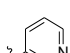
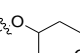
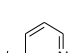
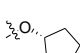
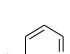
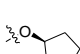
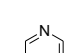
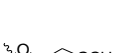
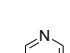

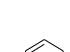
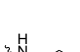
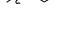
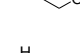
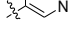
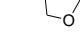
- 1 Janowski, J. Kaus, A. Kovalenko, T.S. Lee, S. LeGrand, P. Li, C. Lin, T. Luchko, R. Luo,
2 B. Madej, AMBER 2016, Univ. Calif. San Fr.
- 3 [43] C. Simmerling, *ff 14SB: Improving the accuracy of protein side chain and backbone*
4 *parameters from ff 99SB*, J. Chem. Theory Comput. 11 (2015), pp. 3696–3713.
- 5 [44] J. Wang, R.M. Wolf, J.W. Caldwell, P.A. Kollman, and D.A. Case, *Development and*
6 *testing of a general amber force field*, J. Comput. Chem. 25 (2004), pp. 1157–1174.
- 7 [45] W.D. Cornell, P. Cieplak, C.I. Bayly and P.A. Kollman, *Application of RESP charges to*
8 *calculate conformational energies, hydrogen bond energies, and free energies of*
9 *solvation*, J. Am. Chem. Soc. 115 (1993), pp. 9620-9631.
- 10 [46] M.W. Mahoney and W.L. Jorgensen, *A five-site model for liquid water and the*
11 *reproduction of the density anomaly by rigid, nonpolarizable potential functions*, J. Chem.
12 Phys. 112 (2000), pp. 8910-8922.
- 13 [47] T. Darden, D. York and L. Pedersen, *Particle mesh Ewald: An $N \cdot \log(N)$ method for Ewald*
14 *sums in large systems*, J. Chem. Phys. 98 (1993), pp. 10089-10092.
- 15 [48] J.P. Ryckaert, G. Ciccotti and H.J.C. Berendsen, *Numerical integration of the cartesian*
16 *equations of motion of a system with constraints: molecular dynamics of n-alkanes*, J.
17 Comput. Phys., 23 (1977), pp. 327–341.
- 18 [49] B.R. Miller, T.D. Mcgee, J.M. Swails, N. Homeyer, H. Gohlke, and A.E. Roitberg,
19 *MPBSA.py: An efficient program for end-state free energy calculations*, J. Chem. Theory
20 Comput. 8 (2012), pp. 3314–3321.
- 21 [50] S. Genheden and U. Ryde, *The MM/PBSA and MM/GBSA methods to estimate ligand-*
22 *binding affinities*, Expert Opin. Drug Discov. 10 (2015), pp. 449–461.
- 23 [51] C.J. Woods, M. Malaisree, S. Hannongbua, A.J. Mulholland, *A water-swap reaction*
24 *coordinate for the calculation of absolute protein–ligand binding free energies*, J. Chem.
25 Phys. 134 (2011), pp. 054114.
- 26 [52] C.J. Woods, M. Malaisree, J. Michel, B. Long, S. McIntosh-Smith and A.J. Mulholland,
27 *Rapid decomposition and visualisation of protein–ligand binding free energies by residue*
28 *and by water*, Faraday Discuss. 169(2014), pp. 477-499.
- 29 [53] D.R. Roe and T.E. 3rd Cheatham, *PTRAJ and CPPTRAJ: Software for processing and*
30 *analysis of molecular dynamics trajectory data*, J. Chem. Theory. Comput. 9 (2013), pp.
31 3084-3095.

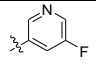
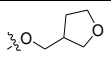
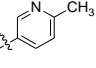
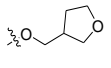
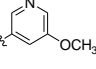
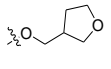
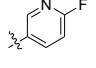
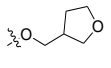
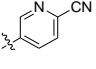
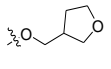
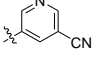
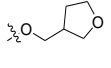
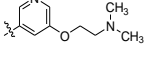
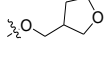
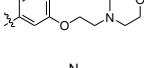
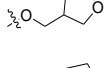
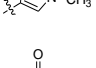
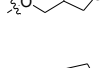
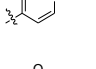
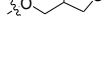
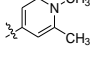
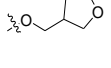
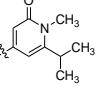
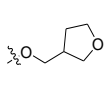
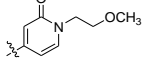
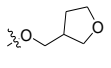
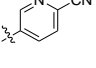
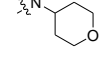
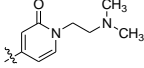
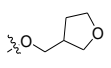
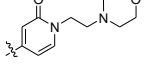
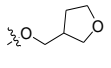
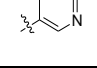
- 1 [54] K. Wendler, J. Thar, S. Zahn and B. Kirchner, *Estimating the hydrogen bond energy*, J.
2 Phys. Chem. A. 144 (2010), 9529-9536.
- 3 [55] A. Daina, O. Michielin and V. Zoete, *SwissADME: a free web tool to evaluate*
4 *pharmacokinetics, drug-likeness and medicinal chemistry friendliness of small molecules*,
5 Sci. Rep. 7 (2017), pp. 42717.
- 6 [56] S.K. Lee, I.H. Lee, H.J. Kim, G.S. Chang, J.E. Chung and K.T. No, *The PreADME*
7 *approach: web-based program for rapid prediction of physico-chemical, drug absorption*
8 *and drug-like properties*, EuroQSAR 2002 designing drugs and crop protectants:
9 *processes, problems and solutions*. Blackwell Publishing, MA, (2003) pp 418–420.
10

1

Table captions2 **Table 1.** Structure and biological activities of thiazole urea core derivatives.

Cpd	Scaffold	R ₁	R ₃	R ₂	IC ₅₀ (nM)	MIC (μM)	log(1/IC ₅₀) ()	log(1/MIC) (C)
1	A	Ethyl		Isopropyl	11	1.3	7.96	5.89
2*	A	Ethyl		Isopropyl	20	3	7.70	5.52
3	A	Ethyl		Isopropyl	16	0.8	7.80	6.10
4	A	Ethyl		Isopropyl	217	12.5	6.66	4.90
5*	A	Ethyl		Isopropyl	2.5	0.2	8.60	6.70
6	A	Ethyl		Isopropyl	23	2	7.64	5.70
7	A	Ethyl		Isopropyl	10	11	8.00	4.96
8	A	Ethyl		Isopropyl	23	10	7.64	5.00
9	A	Ethyl		Isopropyl	6	4	8.22	5.40
10	A	Ethyl		Isopropyl	15	21	7.82	4.68
11	A	Ethyl		Isopropyl	4	4	8.40	5.40
12	A	Ethyl		Isopropyl	20	1.6	7.70	5.80
13	A	Ethyl		Isopropyl	5	0.5	8.30	6.30
14*	A	Ethyl		Isopropyl	5	0.3	8.30	6.52
15	A	Ethyl		Isopropyl	2.5	0.3	8.60	6.52
16	A	Ethyl		H	84	9	7.08	5.05
17	A	Ethyl		Ethyl	30	2	7.52	5.70

18	A	Ethyl		Isopropyl	40	2	7.40	5.70
19	A	Ethyl			40	3	7.40	5.52
20*	A	Ethyl			25	8	7.60	5.10
21	A	Allyl			50	10	7.30	5.00
22	A	Ethyl			40	7.3	7.40	5.14
23	A	Ethyl			14	3	7.85	5.52
24	B	Ethyl		Methoxy	22	2	7.66	5.70
25	B	Ethyl			3.7	0.27	8.43	6.57
26	B	Allyl		H	88	8	7.06	5.10
27	B	Allyl			46	10	7.34	5.00
28	B	Ethyl			25	2.8	7.60	5.55
29	B	Ethyl			12	1.29	7.92	5.89
30	B	Ethyl			5	1.3	8.30	5.89
31	B	Ethyl			9	0.92	8.05	6.04
32*	B	Ethyl			13	1.54	7.89	5.81
33	B	Ethyl			39	0.92	7.41	6.04
34	B	Ethyl			17	0.67	7.77	6.17
35	B	Ethyl			10	0.2	8.00	6.70
36*	B	Ethyl			30	2	7.52	5.70
37	B	Ethyl			30	1	7.52	6.00
38	B	Ethyl			90	3.5	7.05	5.46

39	B	Ethyl			7	0.9	8.15	6.05
40*	B	Ethyl			11	2	7.96	5.70
41	B	Ethyl			8	1.7	8.10	5.77
42*	B	Ethyl			9	0.9	8.05	6.05
43	B	Ethyl			14	0.4	7.85	6.40
44	B	Ethyl			12	0.6	7.92	6.22
45	B	Ethyl			10	4	8.00	5.40
46	B	Ethyl			4	1	8.40	6.00
47	B	Ethyl			10	1.8	8.00	5.74
48	B	Ethyl			1	0.14	9.00	6.85
49	B	Ethyl			4.6	0.14	8.34	6.85
50	B	Ethyl			8	0.53	8.10	6.28
51	B	Ethyl			0.5	0.06	9.30	7.22
52*	B	Ethyl			47	5	7.33	5.30
53	B	Ethyl			3	3.1	8.52	5.51
54	B	Ethyl			2.2	0.6	8.66	6.22
55	C	Allyl		H	160	16	6.80	4.80

1 * test set

2

3

4

1 **Table 2.** The statistical results of HQSAR models.

Activity	Descriptor	q^2	r^2	s	SEE	N	Hologram length
log(1/IC ₅₀)	DA/C/A	0.62	0.91	0.36	0.17	6	353
log(1/MIC)	DA/B/C/A	0.60	0.90	0.41	0.20	6	71

2 A, atoms; B, bonds; C, connections; DA, donor and acceptor; q^2 , leave-one-out (LOO)
3 cross-validated correlation coefficient; r^2 , non-cross-validated correlation coefficient; N,
4 optimum number of components; s, standard error of prediction; SEE, standard error of
5 estimate

6

7

1 **Table 3.** The statistical results of CoMFA and CoMSIA models.

Activity	Descriptor	q ²	r ²	S	SEE	F	N	Fraction
log(1/IC ₅₀)	CoMFA							
	S/E	0.47	0.90	0.42	0.18	96.69	4	40/60
	CoMSIA							
log(1/MIC)	S/E/H/D	0.62	0.98	0.36	0.08	388.93	6	15/33/27/25
	CoMFA							
	S/E	0.33	0.77	0.50	0.30	46.12	3	40/60
log(1/MIC)	CoMSIA							
	S/E/H	0.39	0.73	0.48	0.32	58.40	2	17/38/45

2 S steric field; E electrostatic field; H hydrophobic field; D hydrogen donor field; A
3 hydrogen acceptor field; q², leave-one-out (LOO) cross-validated correlation
4 coefficient; r², non-cross-validated correlation coefficient; N optimum number of
5 components; s standard error of prediction; SEE standard error of estimate; F F-test
6 value

7

8

9

10

1 **Table 4.** Experimental and predicted activities for training and test set in CoMSIA and
 2 HQSAR models.

Cpd.	Scaffold	log(1/IC ₅₀)					log(1/MIC)		
		Exp.	CoMSIA	Res.	HQSAR	Res.	Exp.	HQSAR	Res.
1	A	7.96	8.01	-0.05	7.95	0.00	5.89	5.81	0.08
2*	A	7.70	7.92	-0.22	7.61	0.09	5.52	5.60	-0.08
3	A	7.80	7.86	-0.06	7.98	-0.18	6.10	6.19	-0.09
4	A	6.66	6.57	0.09	6.61	0.06	4.90	4.99	-0.08
5*	A	8.60	8.20	0.40	8.51	0.10	6.70	6.25	0.44
6	A	7.64	7.61	0.03	7.75	-0.11	5.70	5.52	0.18
7	A	8.00	8.05	-0.05	8.03	-0.03	4.96	4.77	0.19
8	A	7.64	7.64	0.00	7.75	-0.11	5.00	5.07	-0.07
9	A	8.22	8.28	-0.06	7.99	0.23	5.40	5.15	0.25
10	A	7.82	7.71	0.12	7.75	0.08	4.68	5.17	-0.49
11	A	8.40	8.43	-0.03	7.97	0.43	5.40	5.68	-0.29
12	A	7.70	7.66	0.03	7.54	0.16	5.80	5.84	-0.04
13	A	8.30	8.29	0.02	8.39	-0.09	6.30	6.25	0.05
14*	A	8.30	8.12	0.19	8.70	-0.40	6.52	6.41	0.12
15	A	8.60	8.60	0.00	8.63	-0.03	6.52	6.59	-0.07
16	A	7.08	7.08	-0.01	7.09	-0.02	5.05	5.10	-0.05
17	A	7.52	7.57	-0.04	7.52	0.00	5.70	5.36	0.34
18	A	7.40	7.40	-0.01	7.76	-0.36	5.70	5.31	0.39
19	A	7.40	7.45	-0.05	7.43	-0.03	5.52	5.46	0.06
20*	A	7.60	7.94	-0.34	7.55	0.05	5.10	5.24	-0.14
21	A	7.30	7.39	-0.08	7.32	-0.02	5.00	5.09	-0.09
22	A	7.40	7.39	0.01	7.49	-0.09	5.14	5.37	-0.24
23	A	7.85	7.85	0.01	7.70	0.16	5.52	5.50	0.02
24	B	7.66	7.65	0.01	7.75	-0.09	5.70	5.91	-0.21
25	B	8.43	8.41	0.03	8.67	-0.24	6.57	6.69	-0.12
26	B	7.06	7.09	-0.03	7.03	0.02	5.10	5.02	0.08
27	B	7.34	7.39	-0.05	7.41	-0.07	5.00	5.25	-0.25
28	B	7.60	7.62	-0.02	7.58	0.03	5.55	5.54	0.02
29	B	7.92	7.90	0.02	7.64	0.28	5.89	5.68	0.21
30	B	8.30	8.33	-0.03	7.98	0.32	5.89	6.07	-0.18
31	B	8.05	7.98	0.07	7.97	0.07	6.04	6.13	-0.09
32*	B	7.89	7.89	0.00	7.78	0.11	5.81	5.93	-0.12
33	B	7.41	7.23	0.17	7.72	-0.31	6.04	5.88	0.16
34	B	7.77	7.77	0.00	7.67	0.10	6.17	6.04	0.13
35	B	8.00	7.94	0.06	8.07	-0.07	6.70	6.57	0.12
36*	B	7.52	7.83	-0.31	7.29	0.23	5.70	5.68	0.02
37	B	7.52	7.57	-0.04	7.39	0.14	6.00	5.97	0.03
38	B	7.05	7.03	0.01	7.05	0.00	5.46	5.54	-0.09
39	B	8.15	8.22	-0.07	8.10	0.06	6.05	6.19	-0.14
40*	B	7.96	8.15	-0.19	7.97	-0.01	5.70	5.95	-0.25

41	B	8.10	8.19	-0.10	8.19	-0.09	5.77	5.72	0.05
42*	B	8.05	8.24	-0.19	7.99	0.05	6.05	6.02	0.03
43	B	7.85	7.93	-0.08	7.97	-0.11	6.40	5.98	0.41
44	B	7.92	7.91	0.01	8.18	-0.26	6.22	6.39	-0.17
45	B	8.00	7.91	0.09	8.14	-0.14	5.40	5.51	-0.12
46	B	8.40	8.41	-0.01	8.30	0.10	6.00	5.82	0.18
47	B	8.00	8.06	-0.06	8.11	-0.11	5.74	5.75	0.00
48	B	9.00	8.75	0.25	8.72	0.28	6.85	6.77	0.08
49	B	8.34	8.36	-0.02	8.41	-0.07	6.85	6.97	-0.12
50	B	8.10	8.24	-0.14	8.16	-0.06	6.28	6.39	-0.11
51	B	9.30	9.22	0.09	9.15	0.16	7.22	7.07	0.15
52*	B	7.33	7.67	-0.35	7.34	-0.01	5.30	5.72	-0.42
53	B	8.52	8.58	-0.05	8.58	-0.05	5.51	5.75	-0.24
54	B	8.66	8.65	0.01	8.58	0.08	6.22	5.97	0.25
55	C	6.80	6.80	-0.01	6.83	-0.04	4.80	4.90	-0.10

1 *test set

2

3

1 **Table 4.** Binding free energy of thiazole urea core derivatives from MM-GBSA and
2 waterswap calculations.

Cpd.	IC ₅₀ (nM)	Energy (kcal/mol)				
		$\Delta G_{Exp.}^*$	ΔH	T ΔS	$\Delta G_{MM-GBSA}$	$\Delta G_{waterswap}$
25	3.7	-11.58	-49.25	-21.24	-28.01	-36.57
26	88	-9.69	-46.56	-25.58	-20.98	-32.12
30	5	-11.40	-49.50	-17.58	-31.92	-33.74
35	10	-10.99	-48.89	-20.73	-28.16	-34.62
51	0.5	-12.77	-59.24	-21.86	-37.38	-45.38
55	160	-9.33	-48.48	-18.69	-29.79	-23.81

3 *Experimental binding free energy ($\Delta G_{Exp.}$) was calculated from $\Delta G_{Exp.} = -RT\ln[IC_{50}]$. Whereas,
4 R is universal gas constant (1.988 kcal/mol) and T is temperature in Kevin (300 K).

5

6

7

8

9

10

11

12

13

14

1 **Table 5.** Predicted biological activities, docking score and pharmacokinetic prediction
 2 of novel thiazole urea derivatives

	Compound 51	D007	D063
HQSAR-IC ₅₀	8.93	8.40	8.01
HQSAR-MIC	6.63	6.21	6.51
Autodock 4.2 docking score (kcal/mol)	-8.62	-9.66	-7.97
BBB	0.02	0.05	0.04
Caco2	38.87	15.72	12.58
CYP2C19 inhibition	Non	Non	Non
CYP2C9 inhibition	Non	Inhibitor	Non
CYP2D6 inhibition	Non	Non	Non
CYP2D6 substrate	Non	Non	Non
CYP3A4 inhibition	Non	Non	Non
CYP3A4 substrate	Substrate	Weakly	Substrate
HIA	94.70	90.50	87.84
MDCK	4.64	0.89	17.99
Pgp inhibition	Non	Non	Non
PPB	49.66	56.20	75.19
Ames test	mutagen	mutagen	mutagen
Carcino Mouse	negative	negative	negative
Carcino Rat	negative	negative	positive
hERG inhibition	low risk	medium risk	low risk

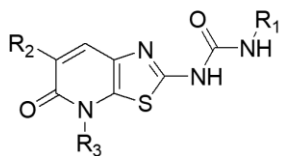
3 BBB: Indicates BB (Cbrain/Cblood) ratio. Value > 0.1 suggested moderate absorption
 4 to CNS
 5 Caco2 permeability: Value of the Pcaco2 (nm/sec) < 4 indicates low permeability.
 6 HIA: Calculated HIA at pH 7.4: Value between 70–100% indicates fair absorption
 7 PPB: Plasma protein binding: Value > 90% indicates strong protein binding
 8 MDCK cell level <25, the molecule is having low permeability

9
 10

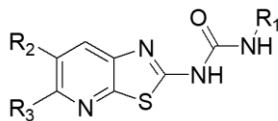
1

Figure captions

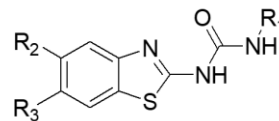
2 **Figure 1.** General structural scaffolds of thiazole urea core derivatives.



Thiazolopyridinone urea
(Scaffold A)



Thiazolopyridine urea
(Scaffold B)

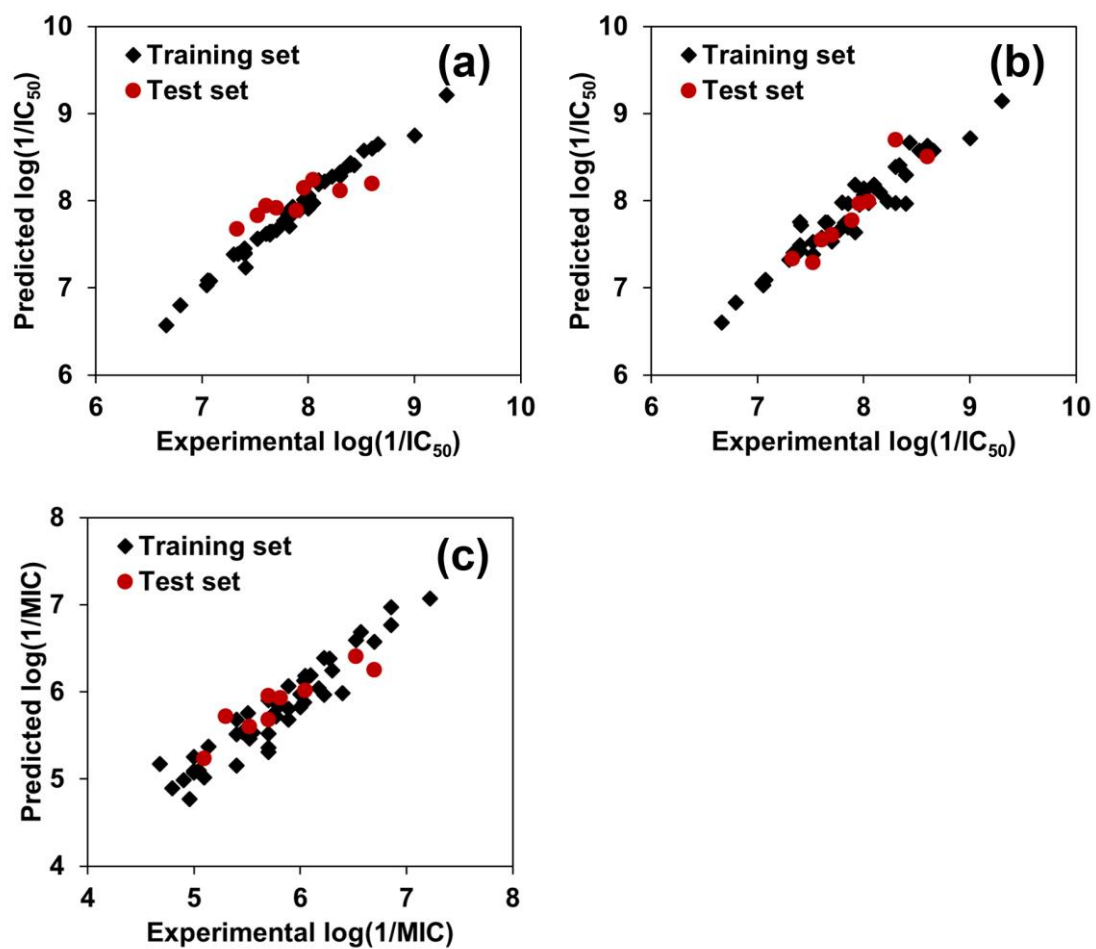


Benzothiazole urea
(Scaffold C)

3

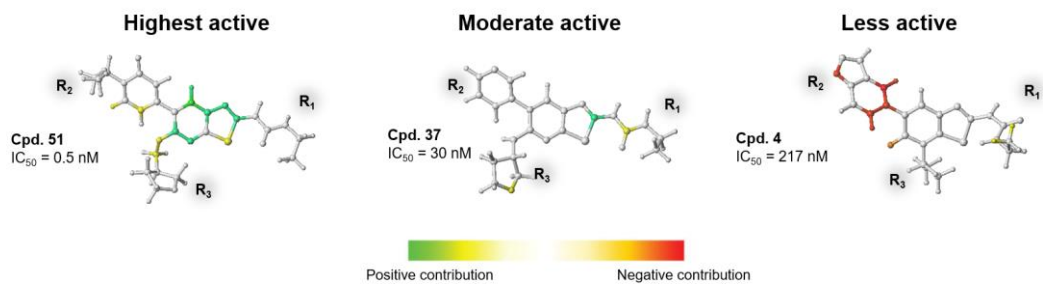
4

- 1 **Figure 2.** Plot of experimental versus predicted biological values from each best IC₅₀
- 2 CoMSIA (a), IC₅₀ HQSAR (b) and MIC HQSAR model (c).



- 3
- 4

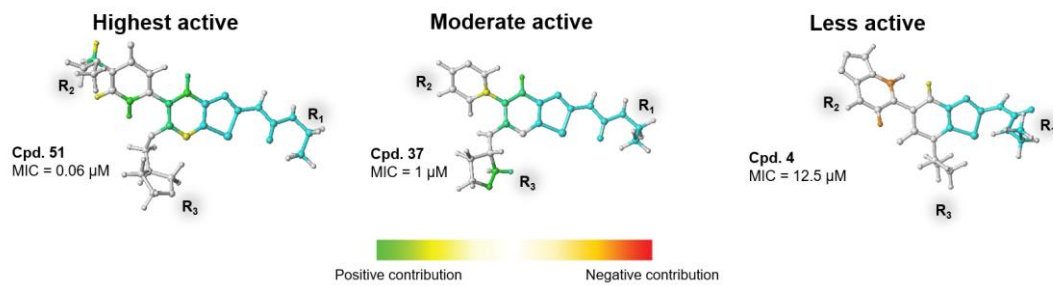
- 1 **Figure 3.** HQSAR contribution of thiazole urea core compounds derived from IC₅₀
- 2 HQSAR model.



3

4

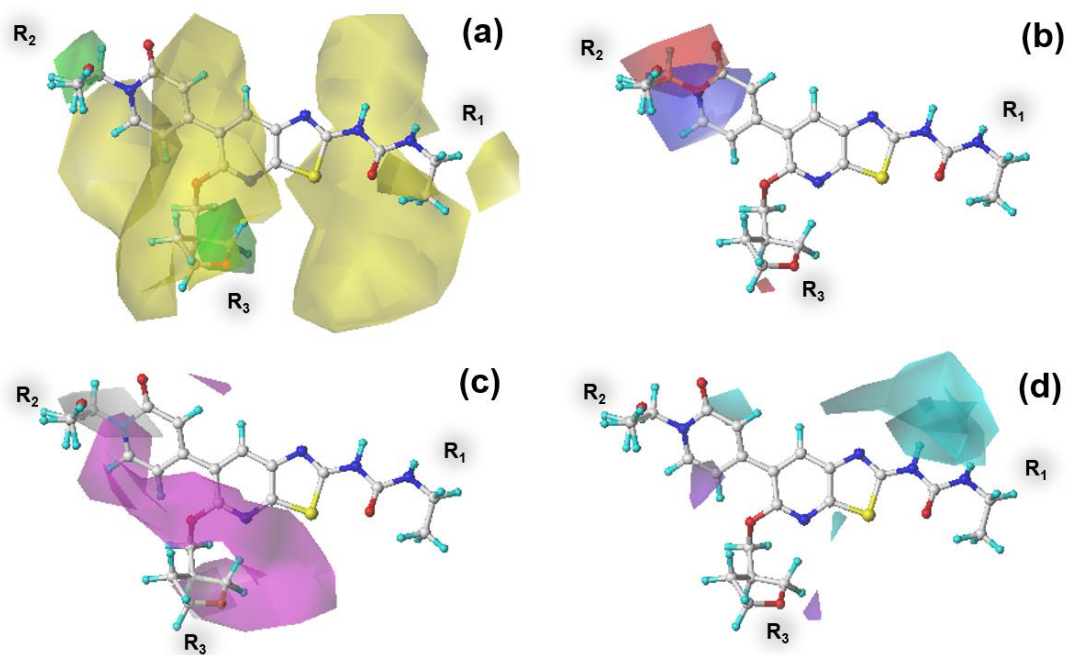
- 1 **Figure 4.** HQSAR contribution of thiazole urea core compounds derived from MIC
- 2 HQSAR model.



3

4

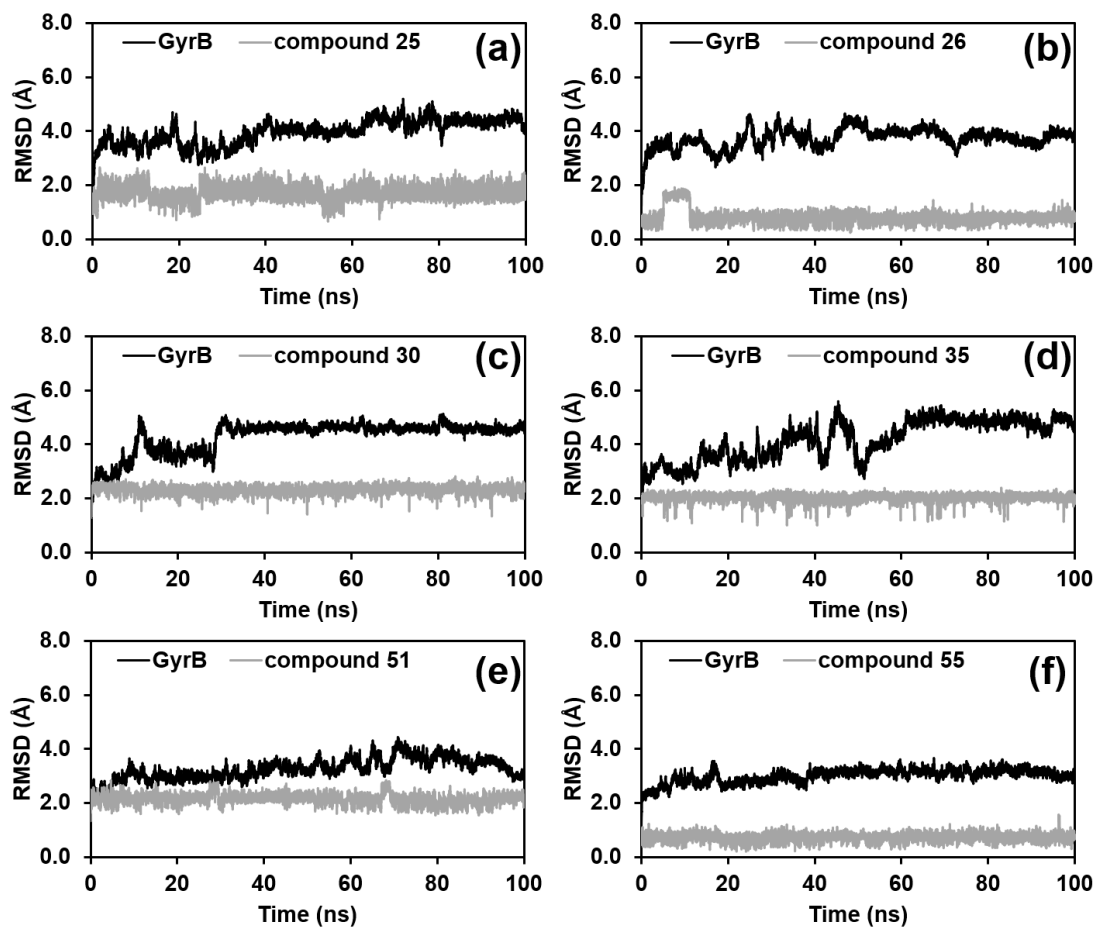
1 **Figure 5.** CoMSIA contour maps derived from the best IC₅₀ CoMSIA model.



2

3

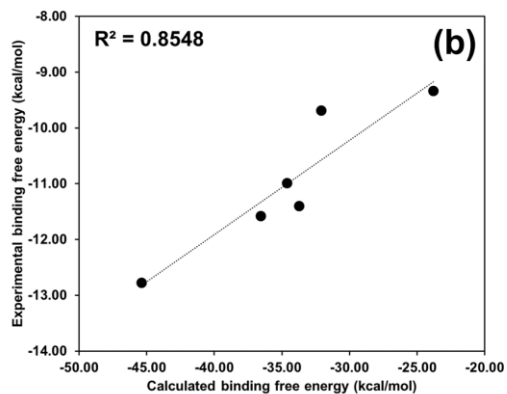
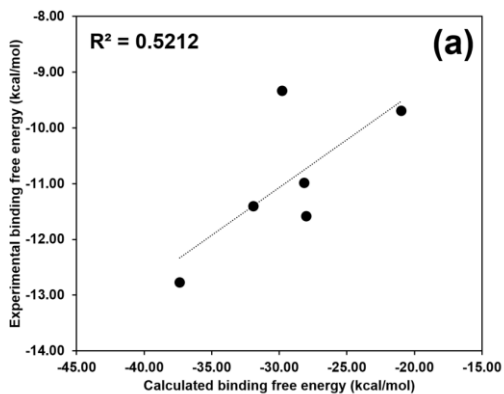
1 **Figure 6.** RMSD plotted of GyrB ATPase complexed with thiazole urea core
2 derivatives; compound **25** (a), compound **26** (b), compound **30** (c), compound **35** (d),
3 compound **51** (e) and compound **55** (f).



4

5

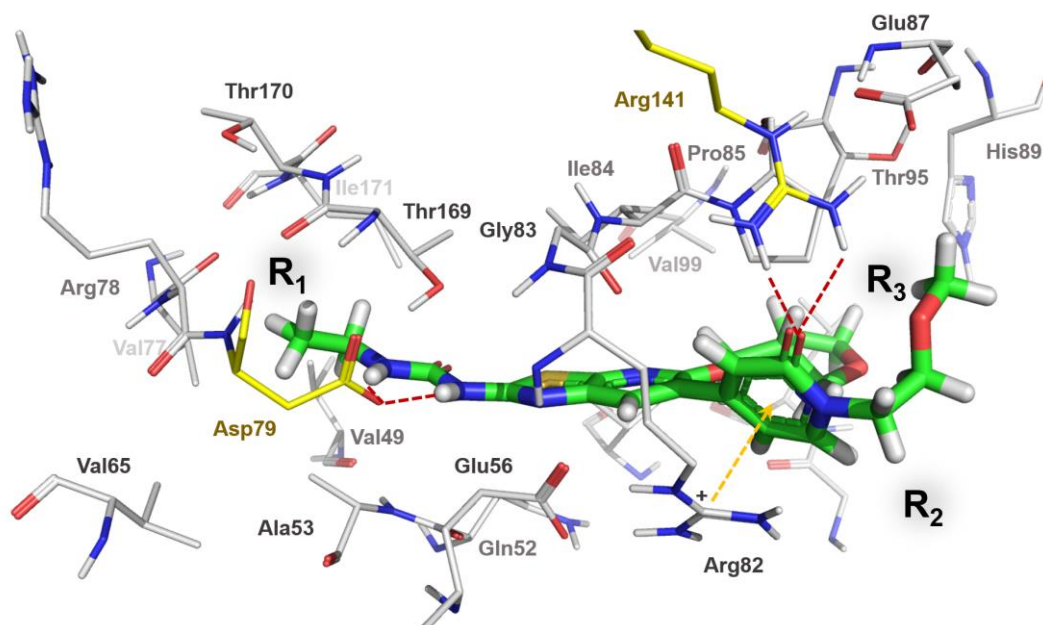
- 1 **Figure 7.** Correlation between experimental binding free energy and calculated binding
2 free energy obtained from MM-GBSA (a) and waterswap calculation (b).



3

4

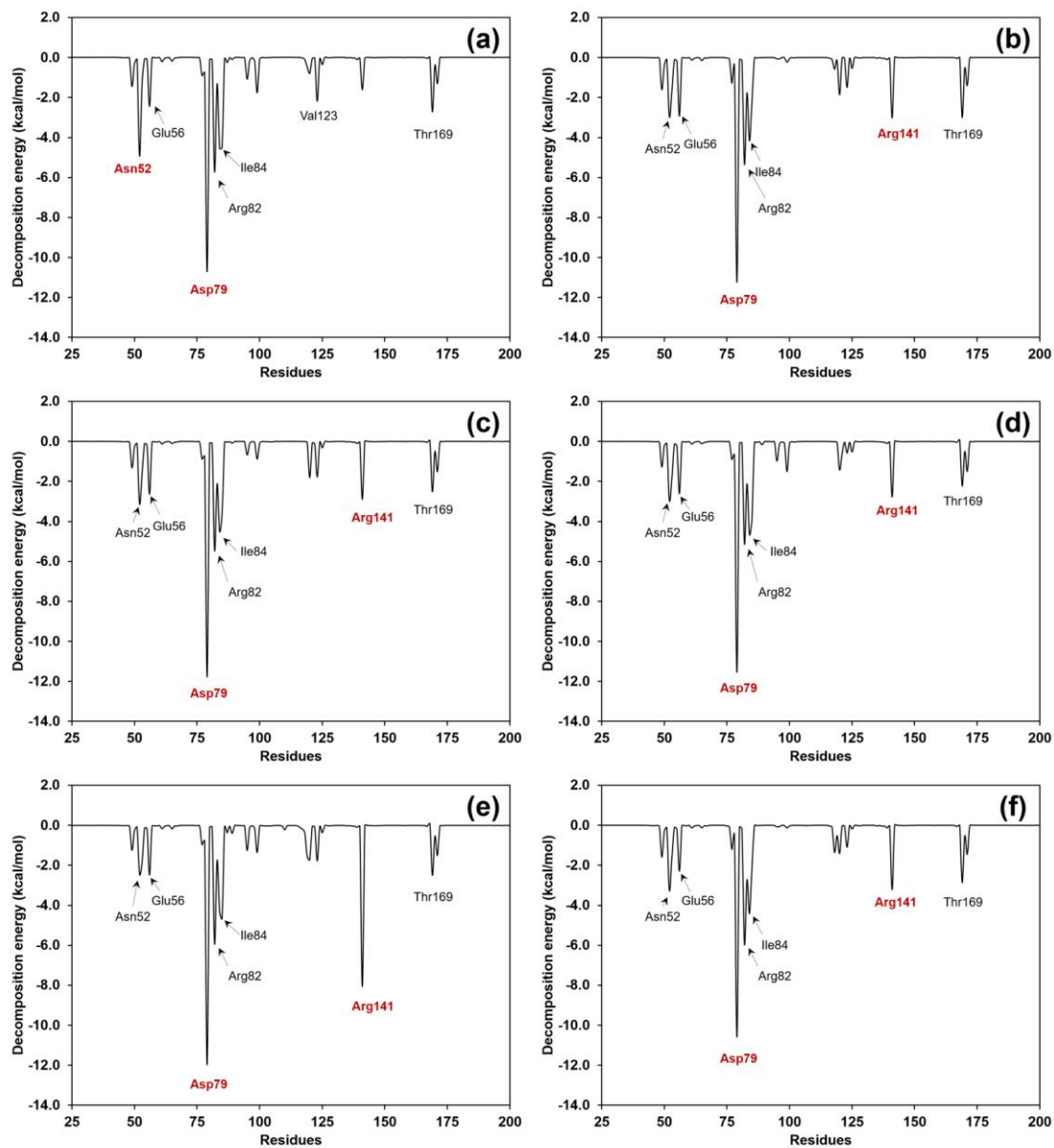
1 **Figure 8.** The binding mode and binding interactions of the highest active compound **51**
2 obtained from MD simulations. Red and yellow dot line indicated hydrogen bond and
3 cation-pi interactions, respectively.



4

5

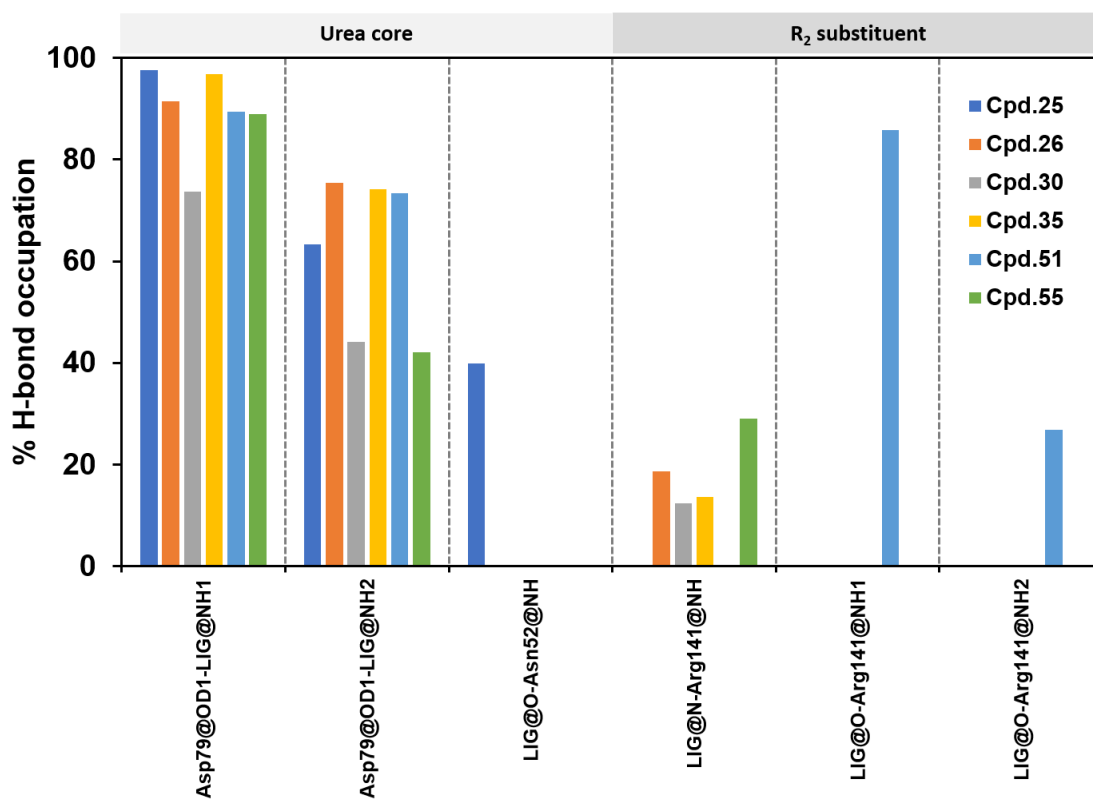
- 1 **Figure 9.** The binding interaction energy profile of thiazole urea core derivatives
- 2 obtained from MM-GBSA calculations.



3

4

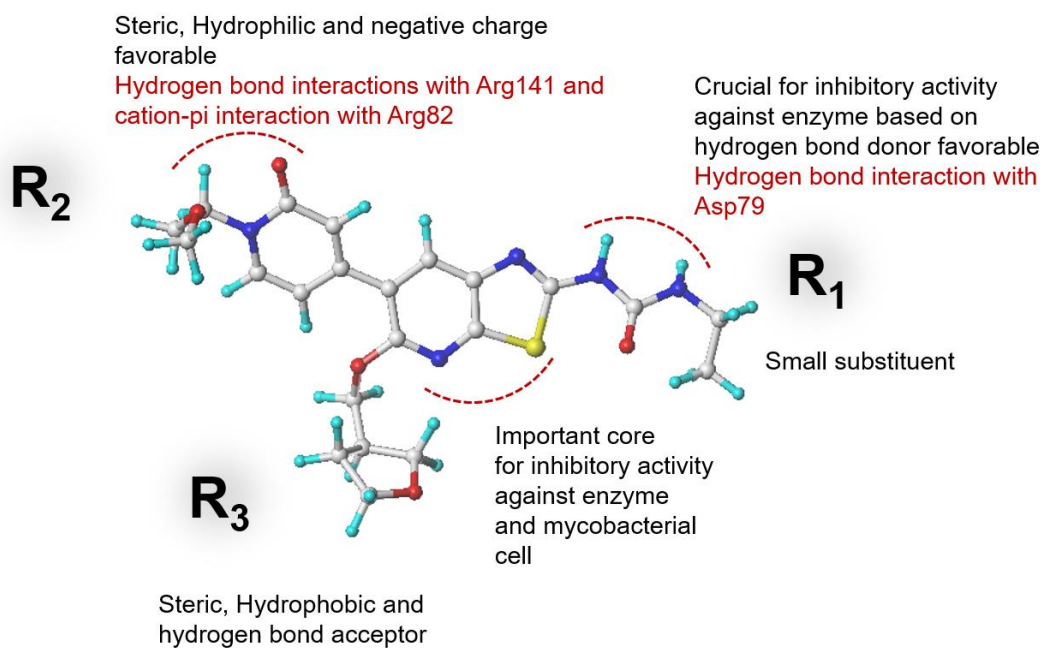
1 **Figure 10.** The hydrogen bond contribution obtained from MD simulations of thiazole
2 urea core derivatives in GyrB ATPase domain.



3

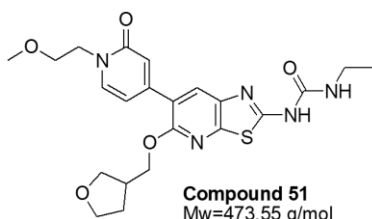
4

- 1 **Figure 11.** The key structural feature of thiazole urea cores for good IC₅₀ and MIC
2 correlation summarized from HQSAR, CoMSIA and MD simulations results. Red and
3 black letters indicate the results obtained from QSAR (HQSAR and CoMSIA) and MD
4 simulations results, respectively.

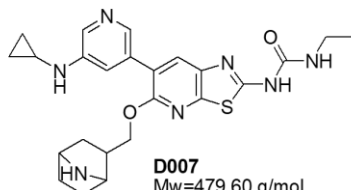


- 5
6

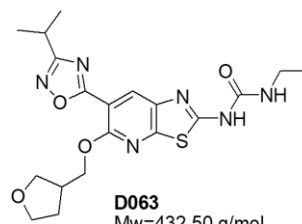
1 **Figure 12.** Structure and drug-like properties of novel thiazole urea derivatives.



Compound 51
Mw=473.55 g/mol
Rotatable bonds = 11
H-bond acceptors = 7
H-bond donors = 2
XlogP3 = 1.39



D007
Mw=479.60 g/mol
Rotatable bonds = 10
H-bond acceptors = 6
H-bond donors = 4
XlogP3 = 3.33

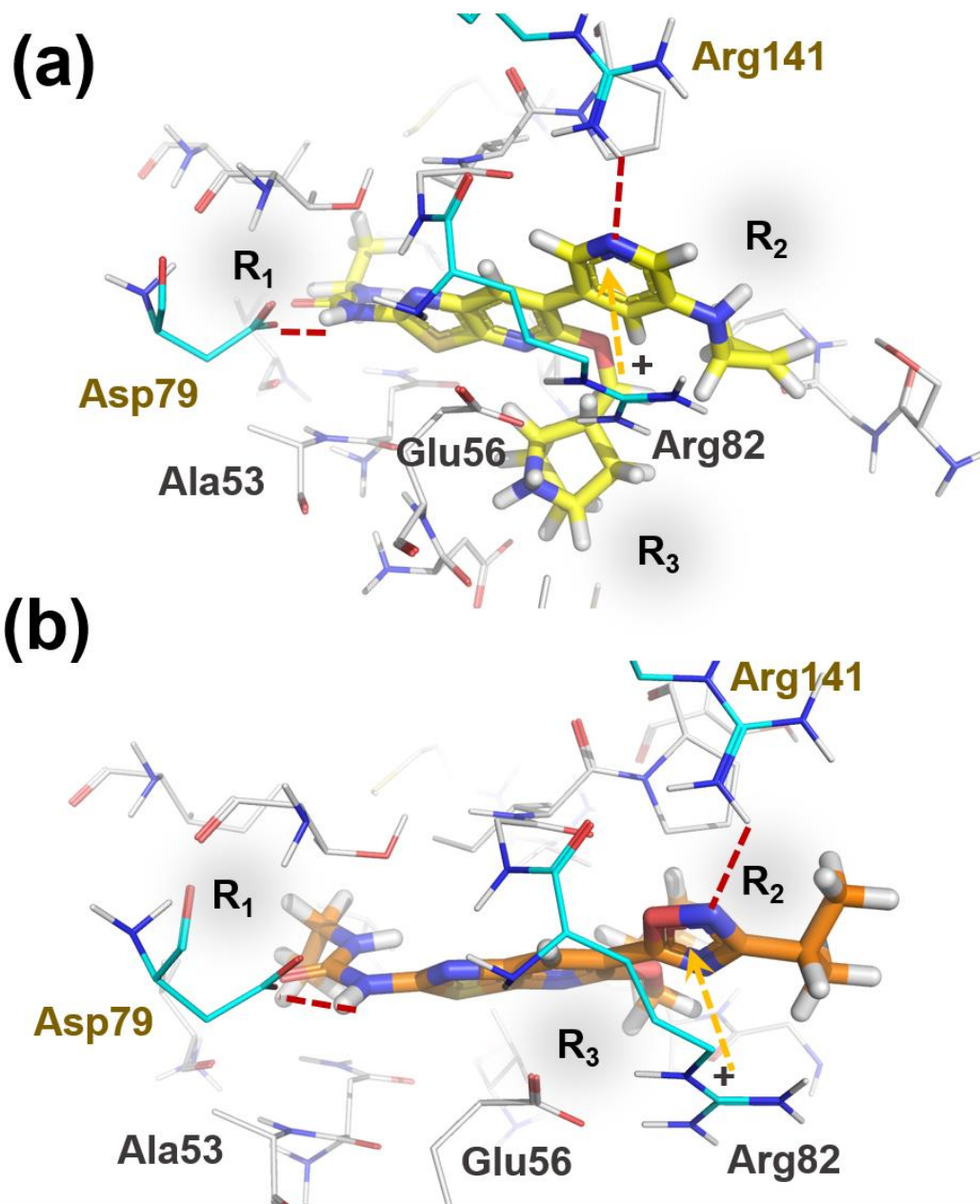


D063
Mw=432.50 g/mol
Rotatable bonds = 9
H-bond acceptors = 8
H-bond donors = 2
XlogP3 = 2.93

2

3

- 1 **Figure 13.** The binding mode and binding interactions of the **D007** (a) and **D063** (b)
- 2 obtained from molecular docking calculations. Red and yellow dot line indicated
- 3 hydrogen bond and cation-pi interactions, respectively.



4
5